Study of intergalactic magnetic fields with methods of gamma-ray astronomy

Alexander Korochkin
(INR RAS Moscow & APC Paris)

Supervisors:
Dmitri Semikoz *(APC Paris)*
Grigory Rubtsov *(INR RAS Moscow)*

Structure of the thesis

Chapter 1: **EBL**

- new EBL model: constraints on parameters underlying it — *arXiv:1712.06579* *MNRAS 2018*
- narrow bump on top of the EBL spectrum — *arXiv:1906.12168* *A&A 2020*

Chapter 2: **ALPs**

- EBL bump from decay of ~1 eV ALPs → new method of constraining ALPs — *arXiv:1911.13291* *JCAP 2020*; *arXiv:1905.02773* *Chin. Phys. C 2022*
- cross check of the "anomalous transparency" of the universe with the most complete list of blazars with reliably measured z — *arXiv:1810.03443* *JCAP 2019*

Chapter 3: **CRPropa, ELMAG, CRbeam** — *arXiv:2201.03996* *Submitted to A&A*

Chapter 4: **IGMF**

- sensitivity of the CTA to strong cosmological IGMF $B \in \mathbf{10^{-12} - 10^{-11}}$ G $\quad$ $Lc \in \mathbf{0.1 - 1}$ kpc — *arXiv:2007.14331* *ApJ 2021* *PoS ICRC2021*
- distinctive features of gamma-ray observations of IGMF with large Lc > **100** Mpc (estimate of the CTA capabilities) — *arXiv:2111.10311* *JETP 2021*
- baryonic feedback effect in gamma-ray measurements of IGMF — *arXiv:2106.02690* *A&A 2022*

Magnetic field in galaxies and galaxy clusters

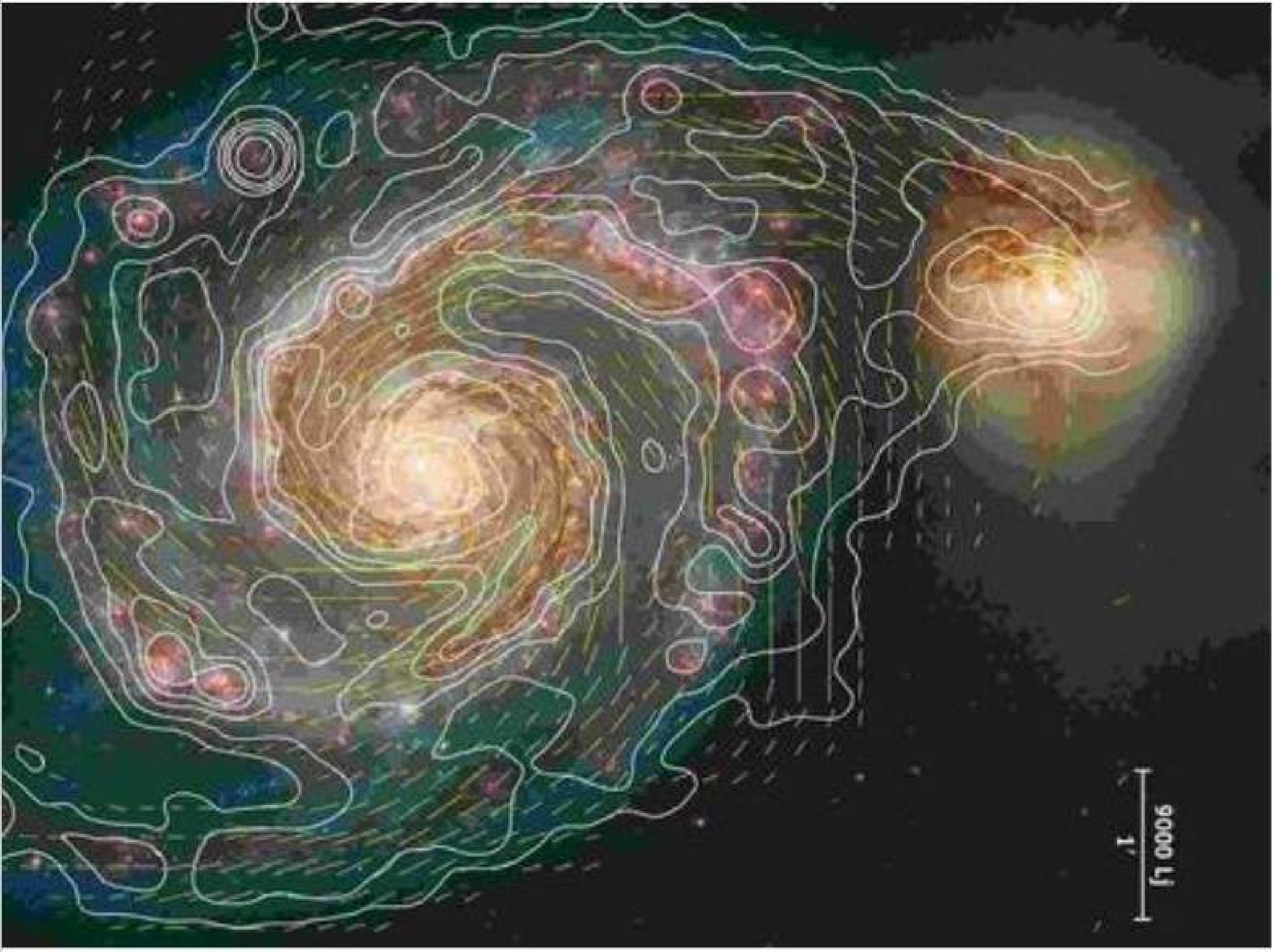

Dynamo amplification

Seed field?

Many independent observations indicate that the magnetic field in our Galaxy, other galaxies and galaxy clusters is on the order of 1 μG

Generation of the seed field

Seed field should be present in galaxies at the dawn of their formation

Generation in the Early Universe

Inflation

QED or QCD phase transitions in the Early Universe

Astrophysical origin – Biermann battery processes

Magnetic field in galaxies has been significantly reprocessed and thus the information about the parameters of the seed field has been lost.

New “window” to the Early Universe

Primordial MF may survive in the voids of LSS

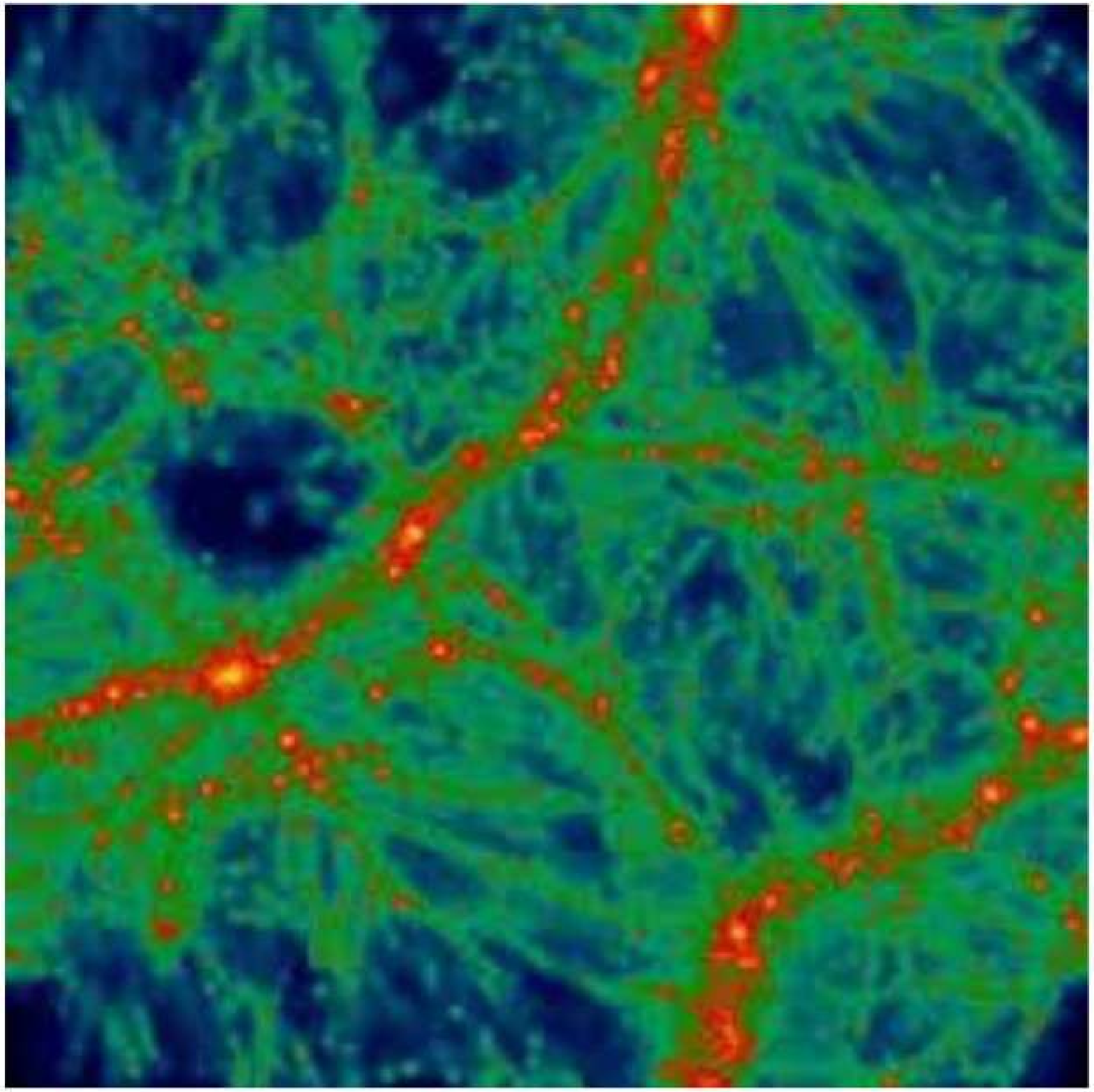

Properties of IGMF

- Turbulent
- Strength B
- Correlation length λ
- Power spectrum

IGMF – intergalactic magnetic field

Upper limits on IGMF strength

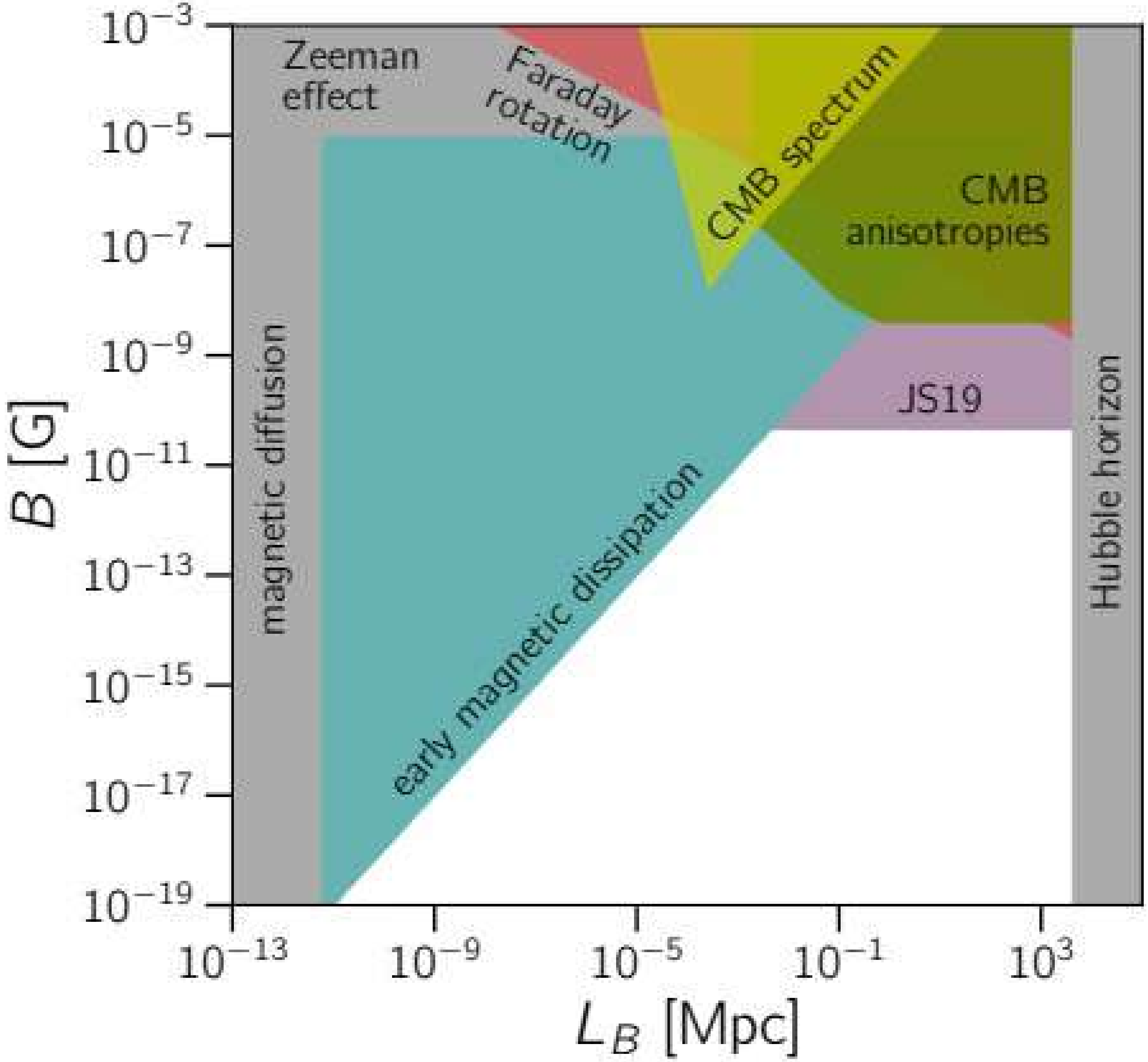

Lower limits on IGMF strength: gamma-ray propagation

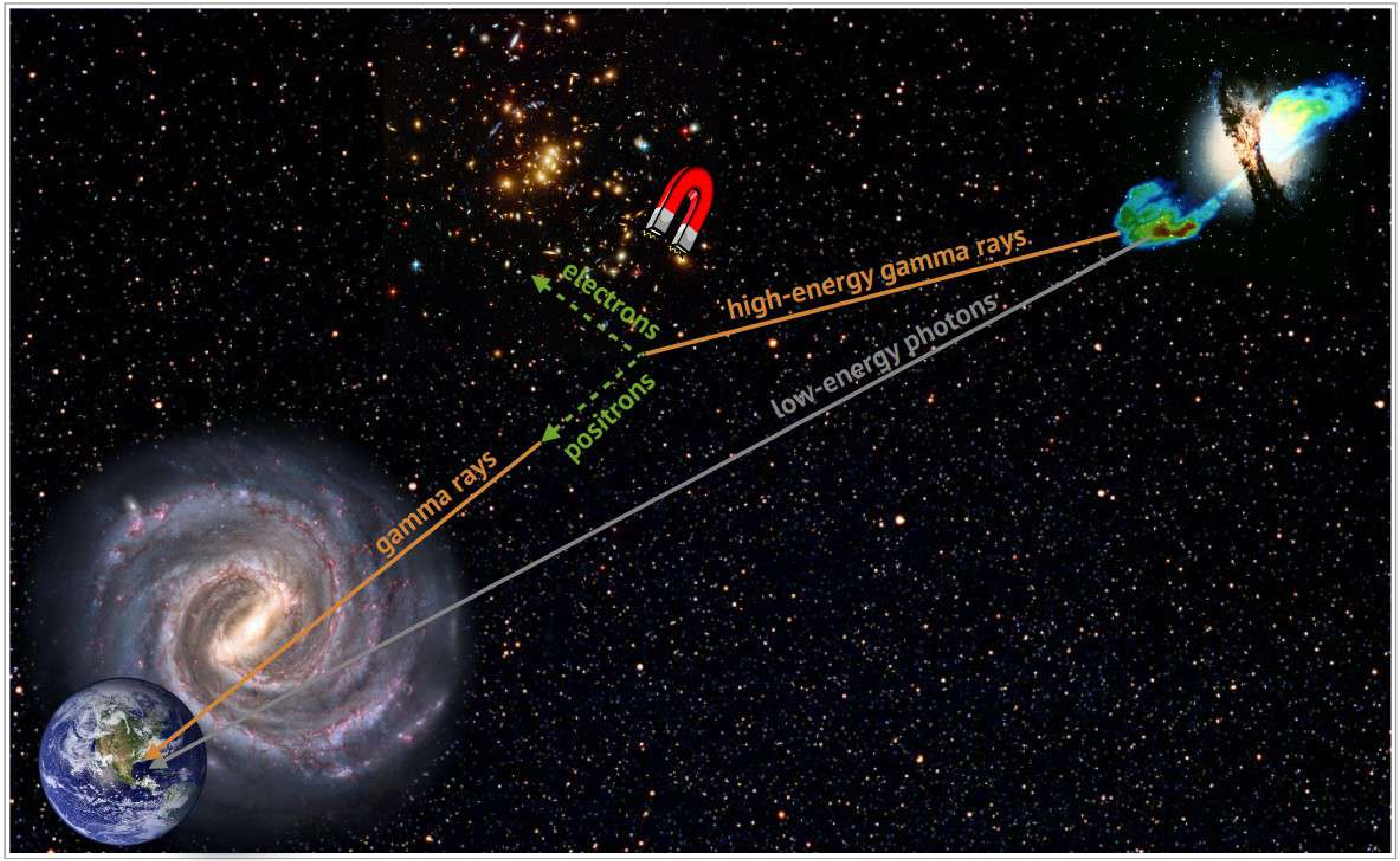

Pic from Rafael Alves Batista slides

Gamma-ray mean free path

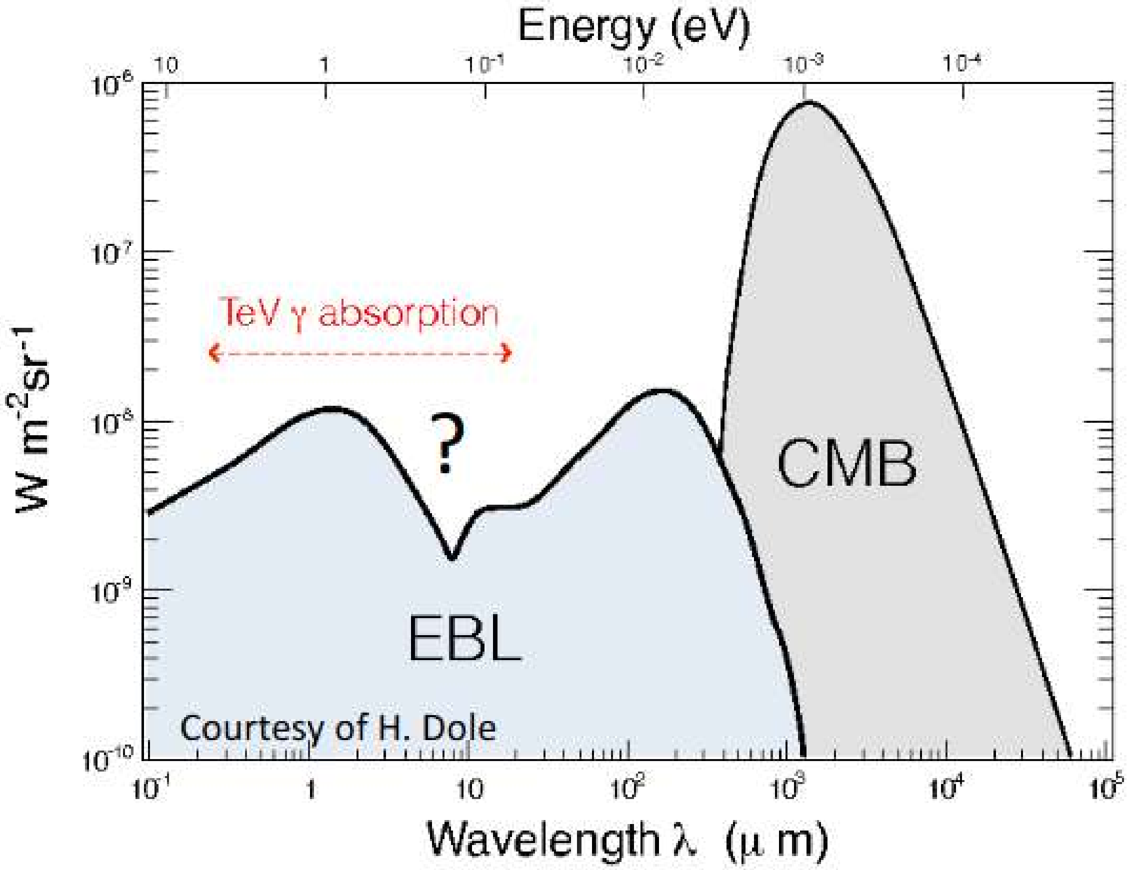

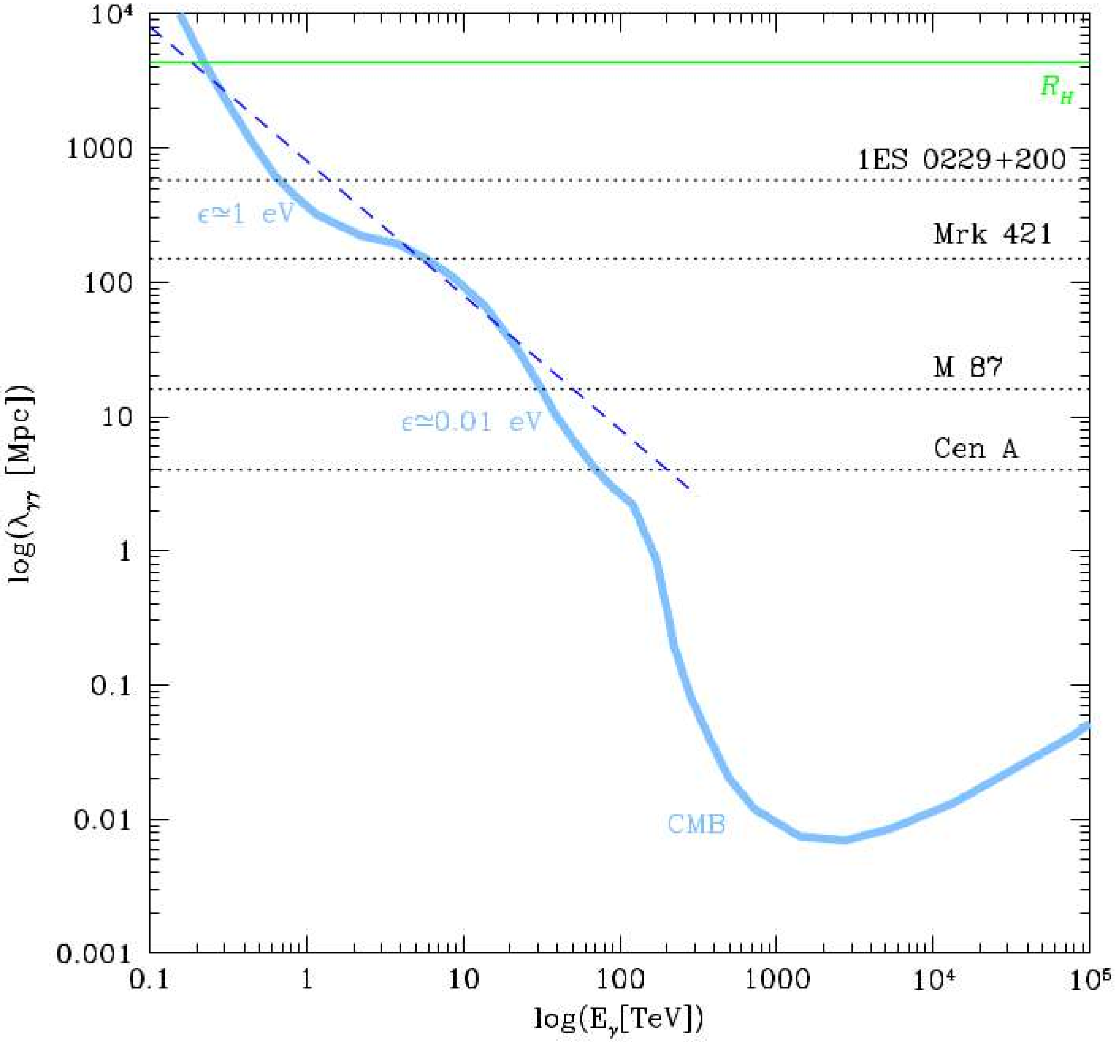

Gamma-ray technique for measurement of IGMF

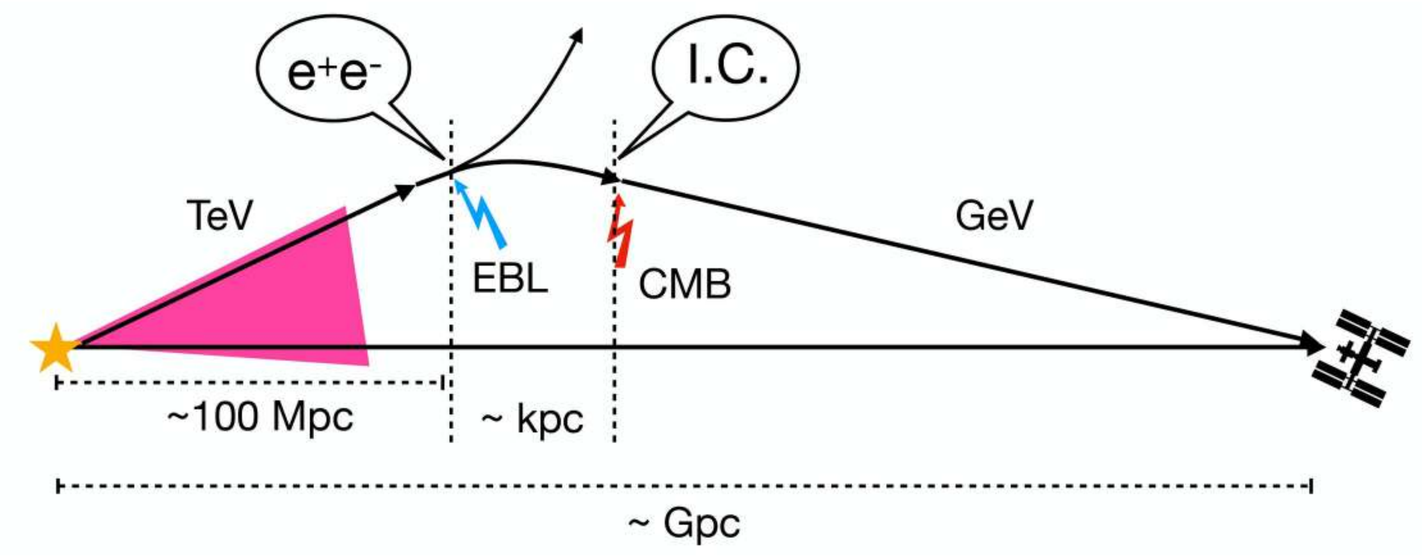

pic from T.Vachaspati arXiv:2010.10525

1) $\gamma_{HE}\ \gamma_b$ –> e+e-

2) γ_b e- –> γ_{HE} e-

Pair production process creates **electron-positron pairs** whose deflections are proportional to the strength of the magnetic field.

Then **secondary gamma rays** are produced by **inverse Compton scattering** off CMB photons.

If the magnetic field is sufficiently strong, the **extended emission** will appear around initially point source.

Electromagnetic cascade

A.Neronov, D.Semikoz arXiv:astro-ph/0604607

What is the maximum IGMF strength that can be probed with the CTA?

Nondetection of cascade component in the GeV band sets lower limit on the IGMF →

IGMF was sufficiently strong to deflect secondary electrons

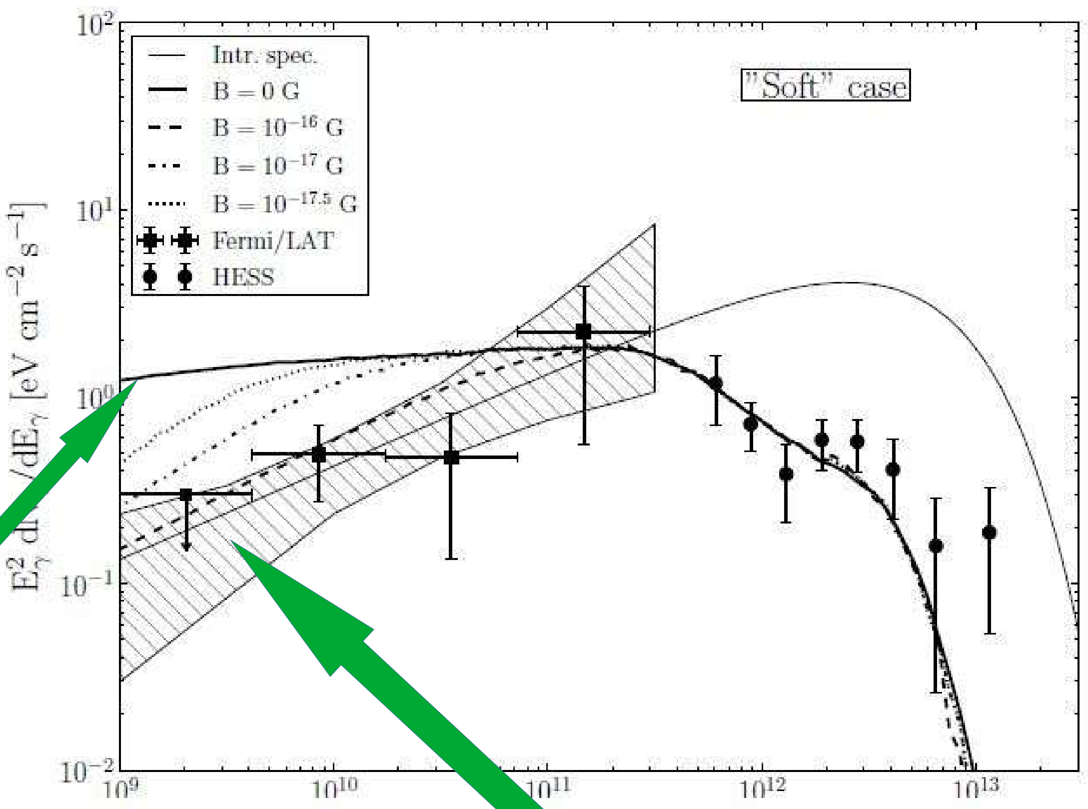

Vovk I, Taylor A.M, Semikoz D, Neronov A
arXiv:1112.2534

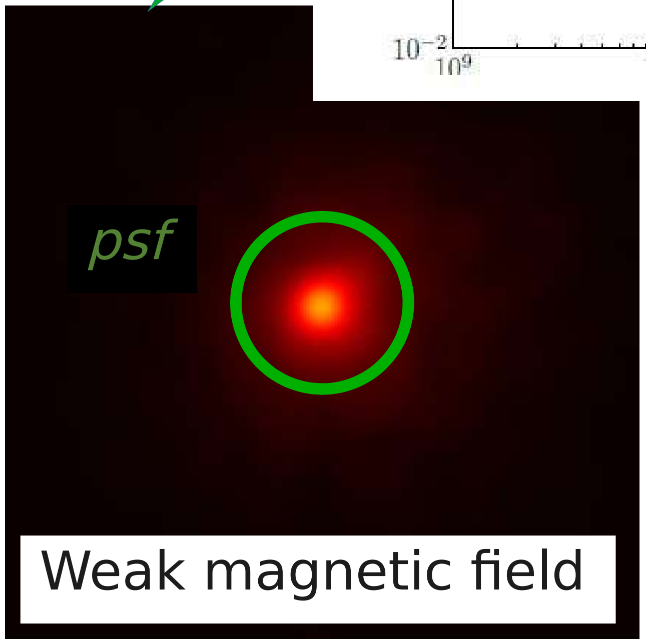

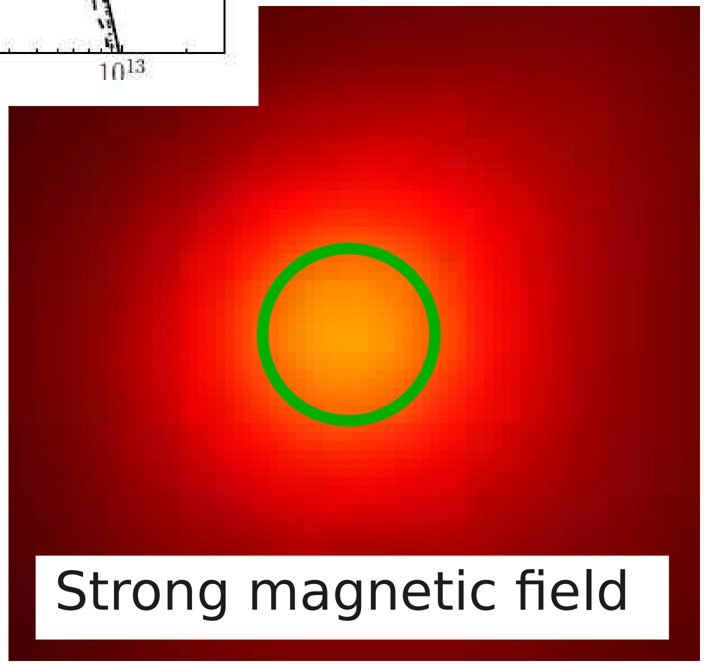

Lower limits on IGMF strength

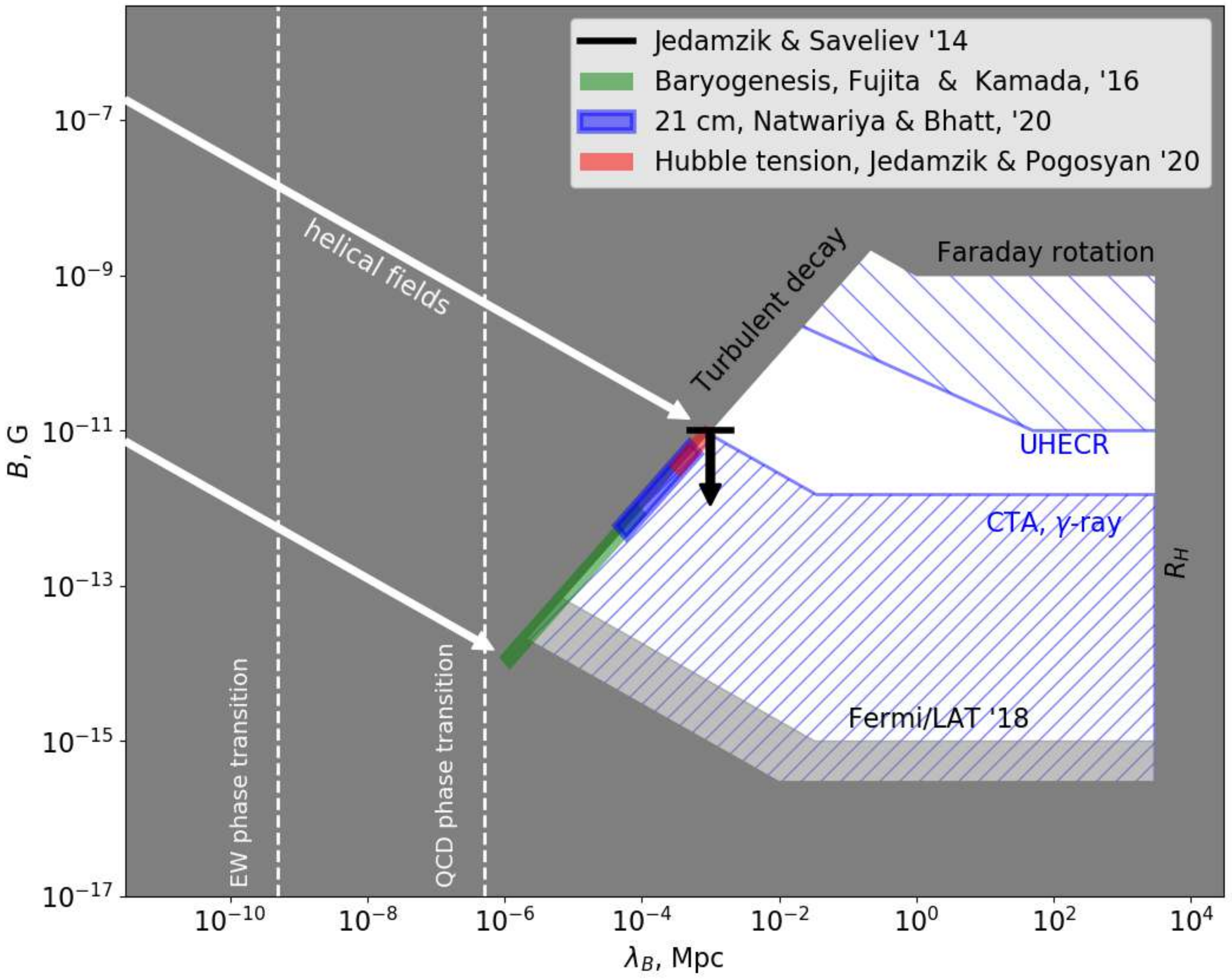

Motivation

The additional baryon inhomogeneities, induced by primordial magnetic fields present in the plasma prior to recombination can relieve Hubble tension.

Required [B ~ 10^{-11} G; λ ~ 1 kpc]

K.Jedamzik, L.Pogosian, arXiv: *2004.09487*

An excess opacity of the universe in the redshift range 15<z<20, reported by the EDGES experiment. Magnetic field strength, which is required to explain EDGES data is

[B: 5*10^{-13} - 6*10^{-12} G]

P.Natwariya, J.Bhatt, arXiv: *2001.00194*

The presence if a helical magnetic field can enable an explanation of the baryon asymmetry of the universe within the standard model of particle physics

[B: 10^{-14} - 10^{-12} G]

T.Fujita, K.Kamada, arXiv: *1602.02109*

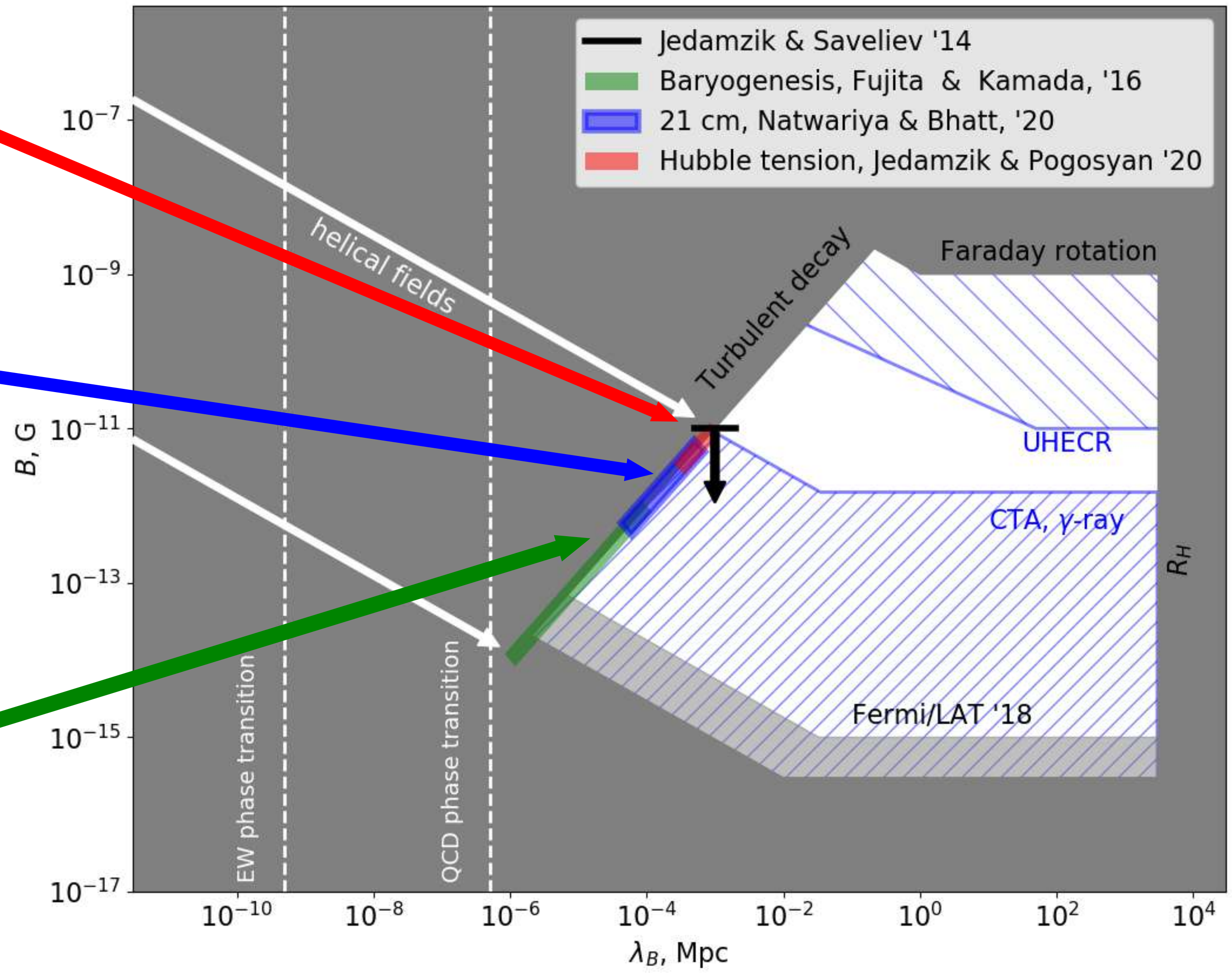

NANOGrav: stochastic gravitational wave background (SGWB)

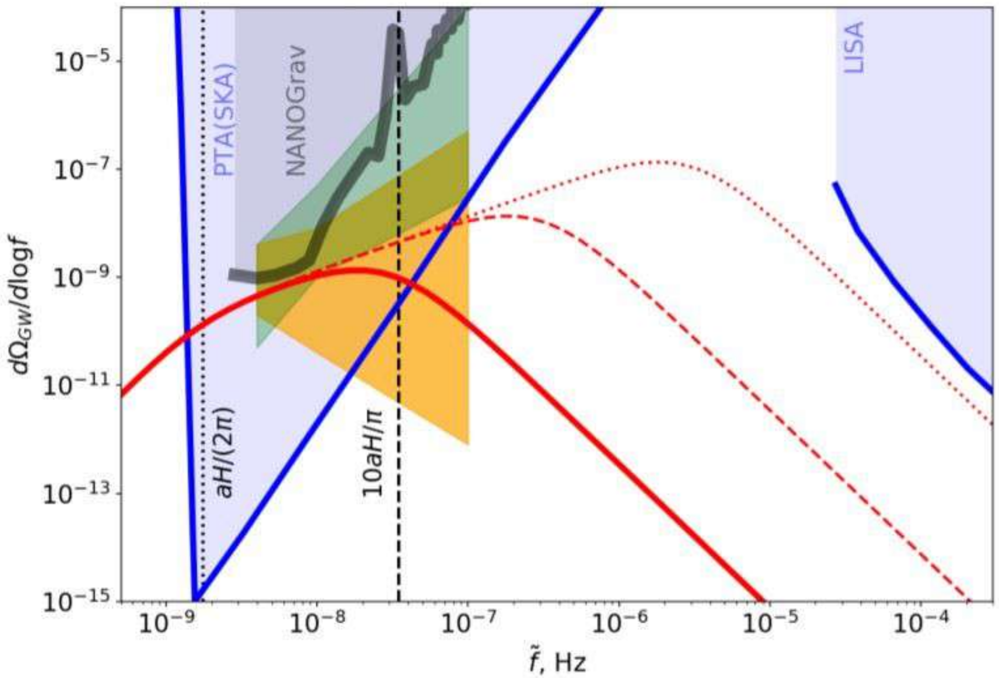

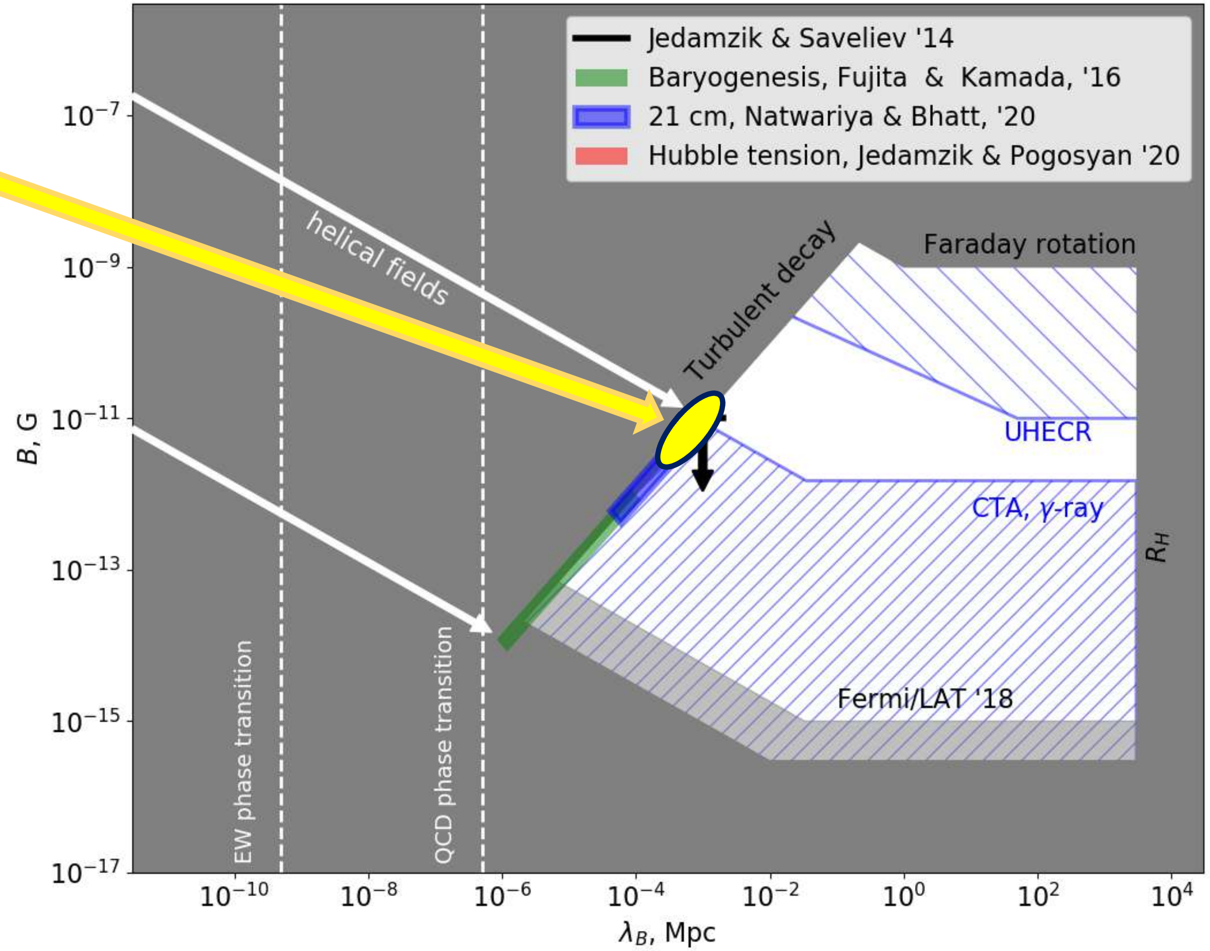

Magnetic field generated at QCD phase transition

Z. Arzoumanian et al, arXiv:2009.04496

A.Neronov, A. Roper Pol, C. Caprini, D.Semikoz, arXiv:2009.14174

Requirements to probe B~10^{-12} - 10^{-11} G

- Large primary point-source power in the **100 TeV** energy range

- strong B - high enery of secondaries

- Detectability of extended emission in the multi-TeV energy range (**nearby source**)

- Favorable local environment – **absence of large magnetized bubble blown by the host galaxy and large filamentary system of magnetized bubbles in the direction toward Earth** (presence of primordial IGMF in the several Mpc region around the source)

$$\lambda_{\gamma 0} \simeq 2.5 \left[\frac{E_{\gamma 0}}{100\ \mathrm{TeV}}\right]^{-1.6} \ \mathrm{Mpc}$$

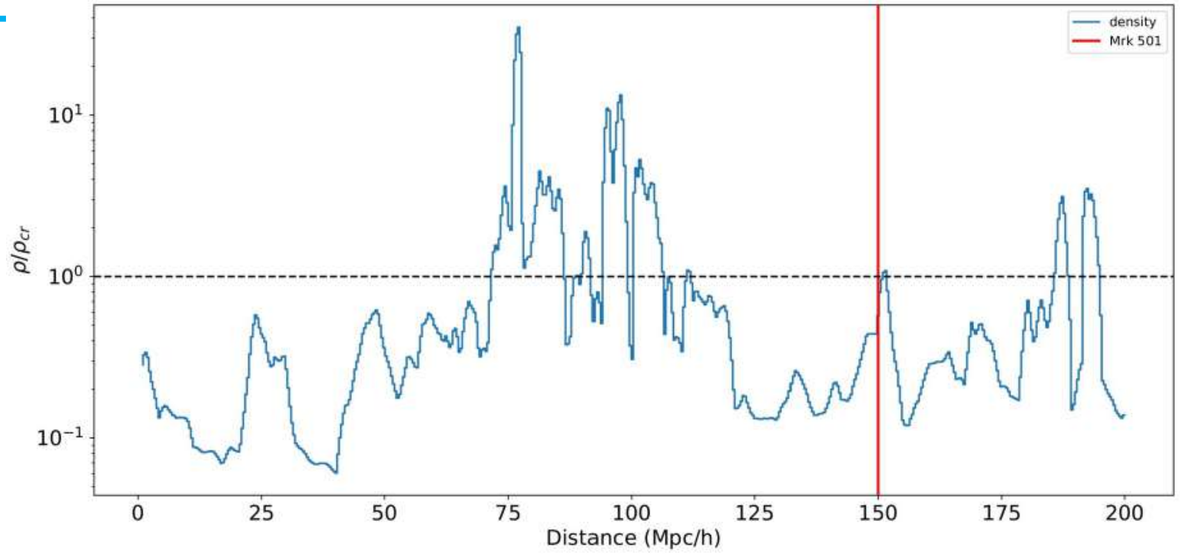

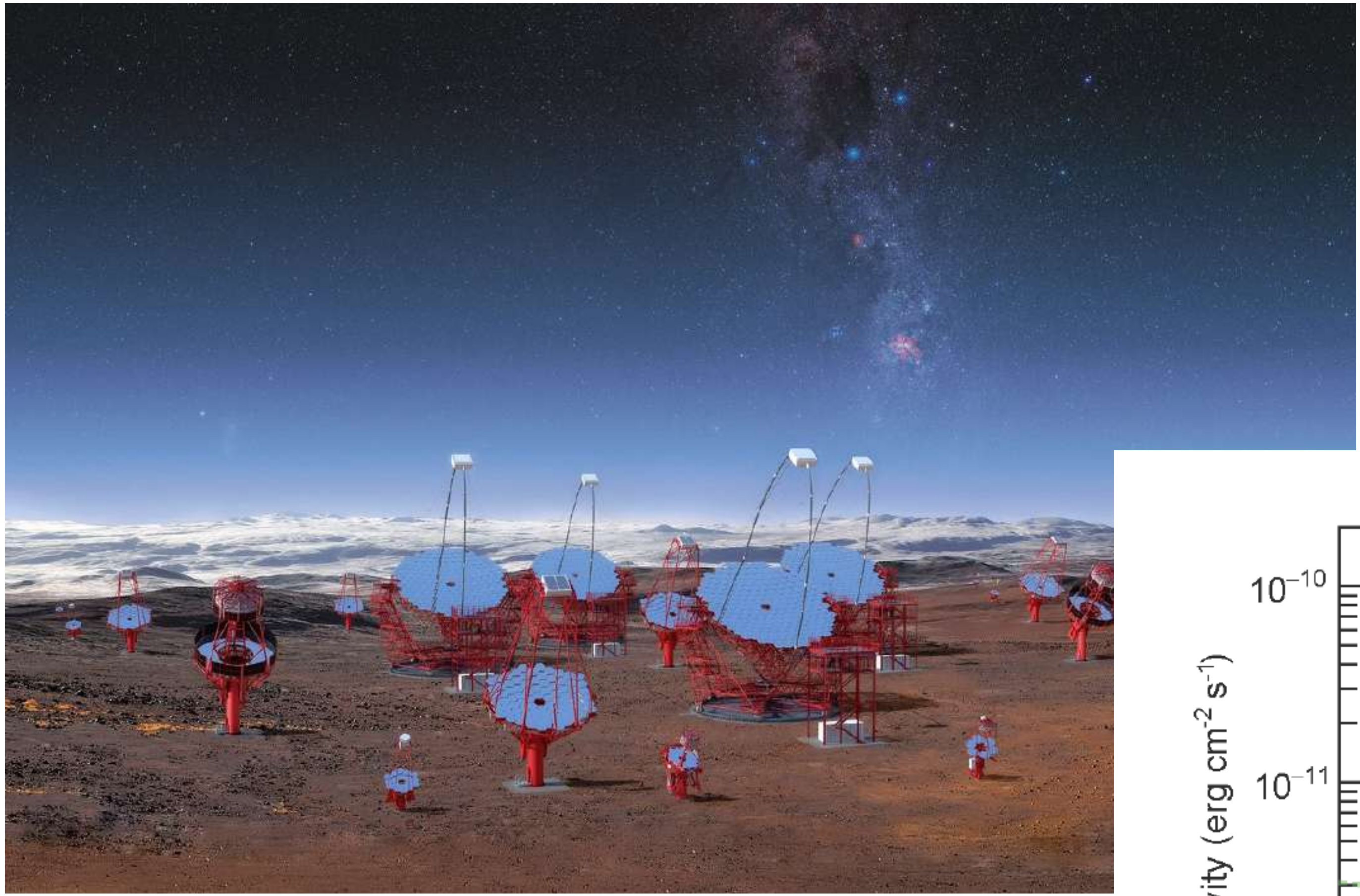

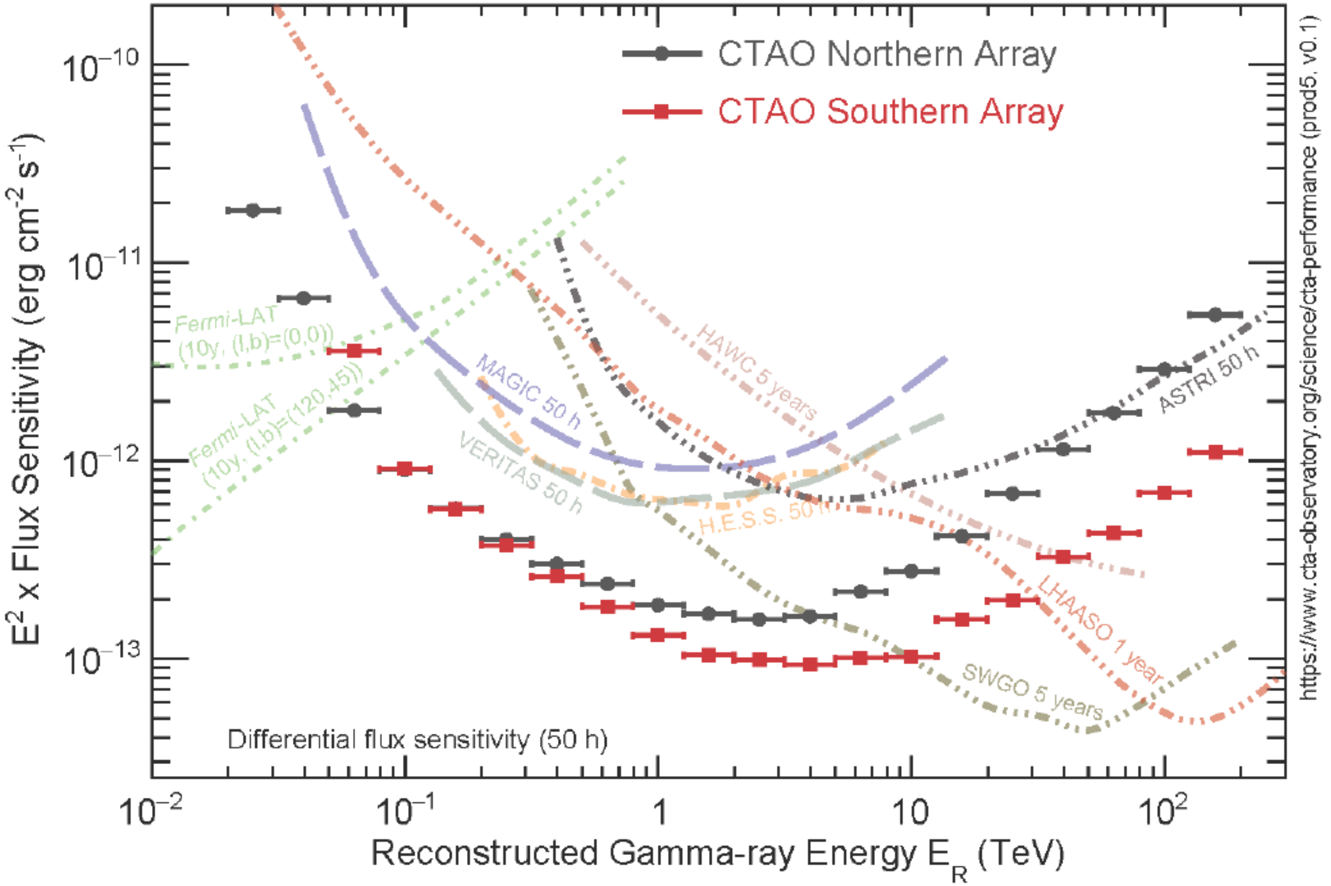

CTAO Northern Array
CTAO Southern Array
E² x Flux Sensitivity (erg cm⁻² s⁻¹)
Reconstructed Gamma-ray Energy E_R (TeV)
Differential flux sensitivity (50 h)
Fermi-LAT (10y, (l,b)=(0,0))
Fermi-LAT (10y, (l,b)=(120,45))
MAGIC 50 h
VERITAS 50 h
H.E.S.S. 50 h
HAWC 5 years
LHAASO 1 year
SWGO 5 years
ASTRI 50 h
https://www.cta-observatory.org/science/cta-performance (prod5, v0.1)

Suitable source: nearest blazar Mrk501

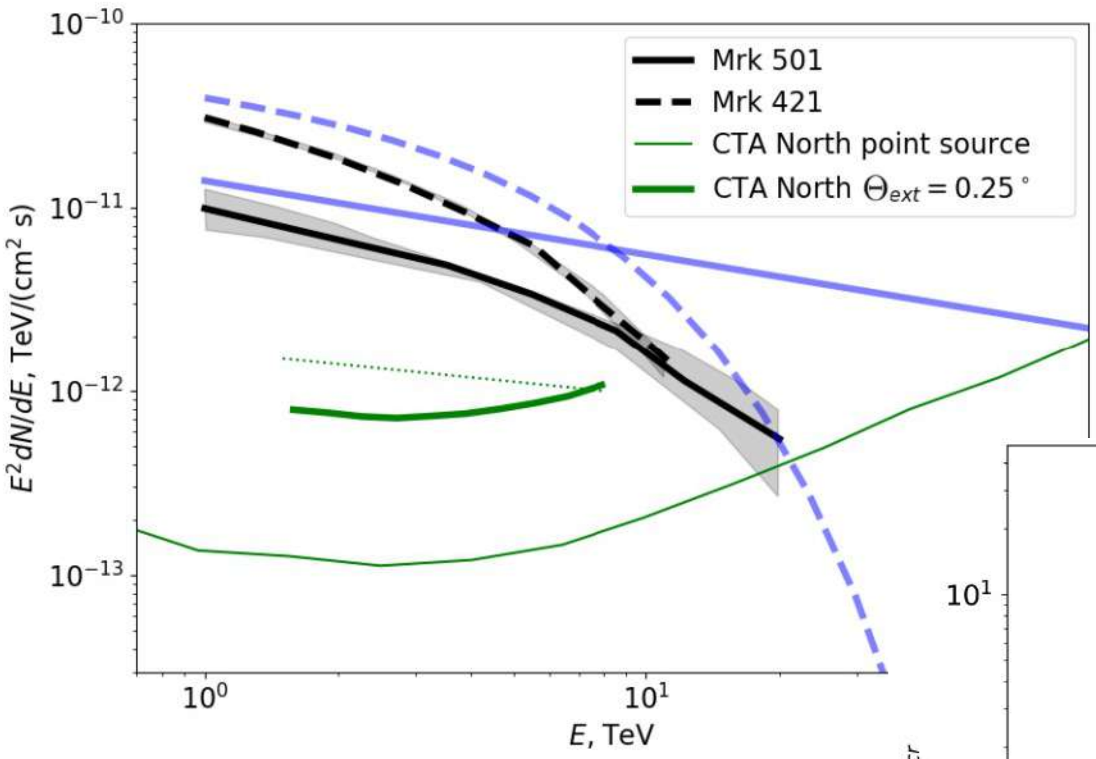

O.Kalashev, AK, A.Neronov, D.Semikoz

arXiv:2007.14331

- Dark matter density profile along the line of sight toward Mrk 501 based on constained simulation of the LSS

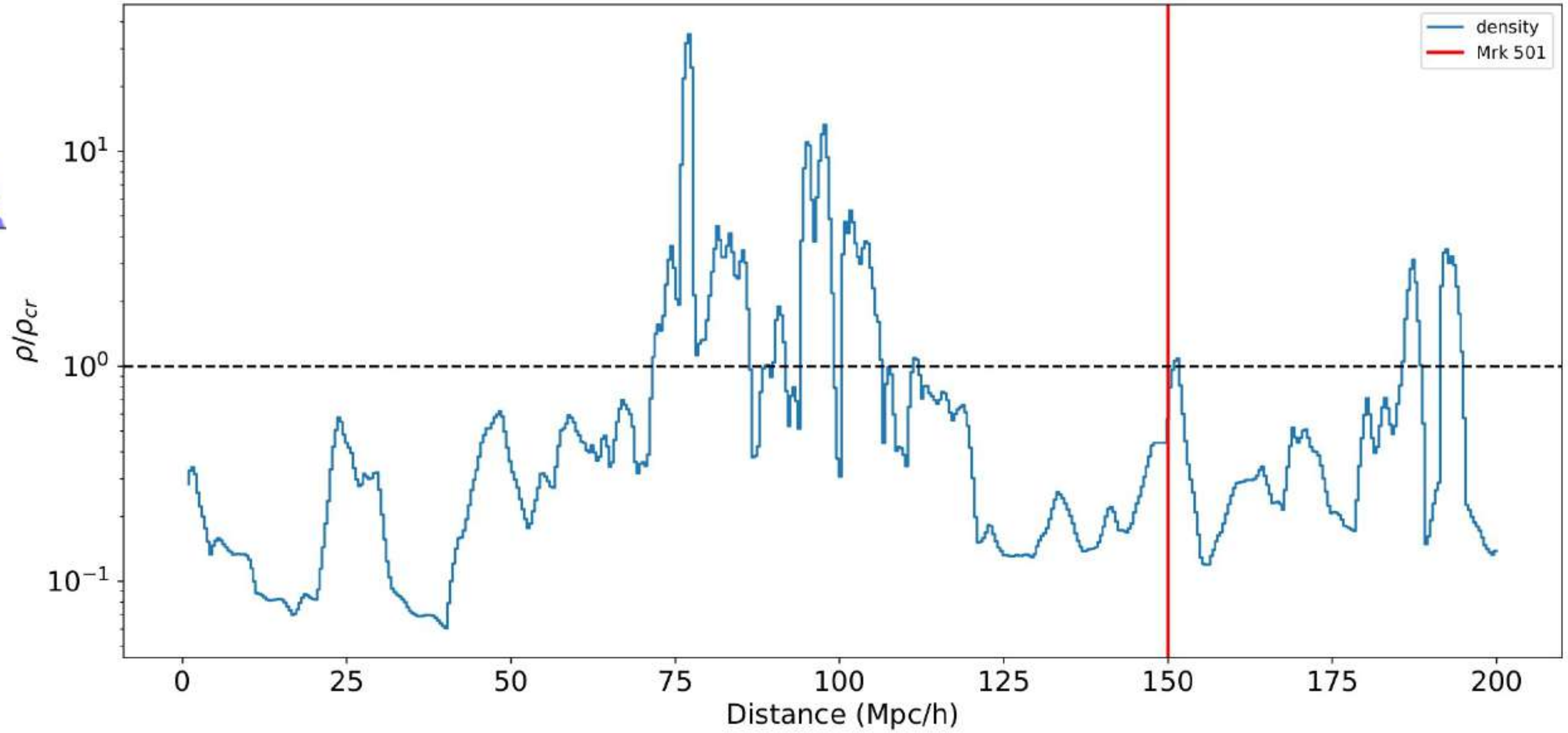

- z = 0.034
- No cutoff up to 20 TeV
- We extended spectrum up to 100 TeV

Angular spectrum

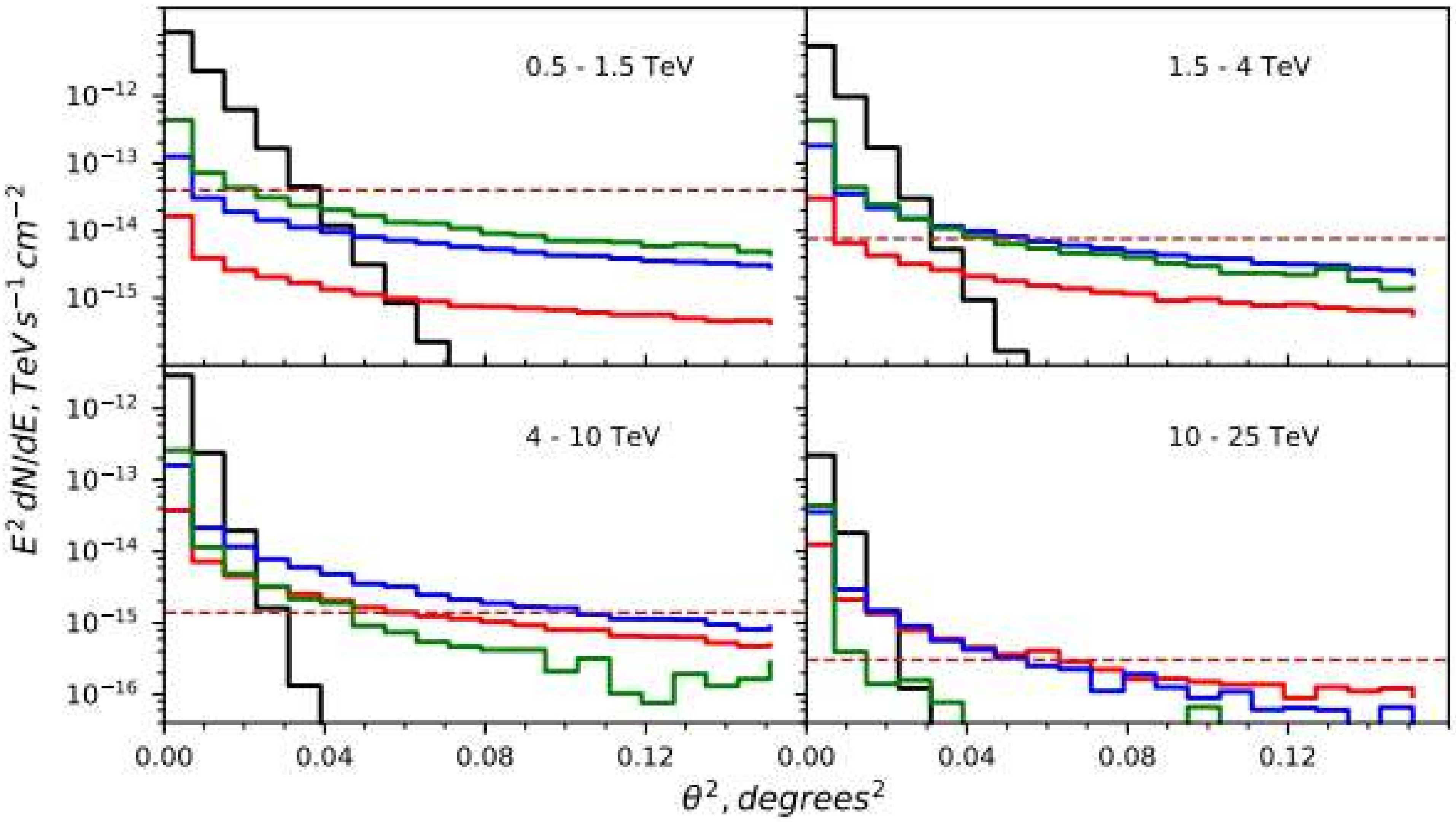

- Green lines – 10^{-12} G
- Blue – $3*10^{-12}$ G
- Red – 10^{-11} G
- Brown – background level
- Black – psf of the CTA

O.Kalashev, AK, A.Neronov, D.Semikoz

arXiv:2007.14331

Results

O.Kalashev, AK, A.Neronov, D.Semikoz
arXiv:2007.14331

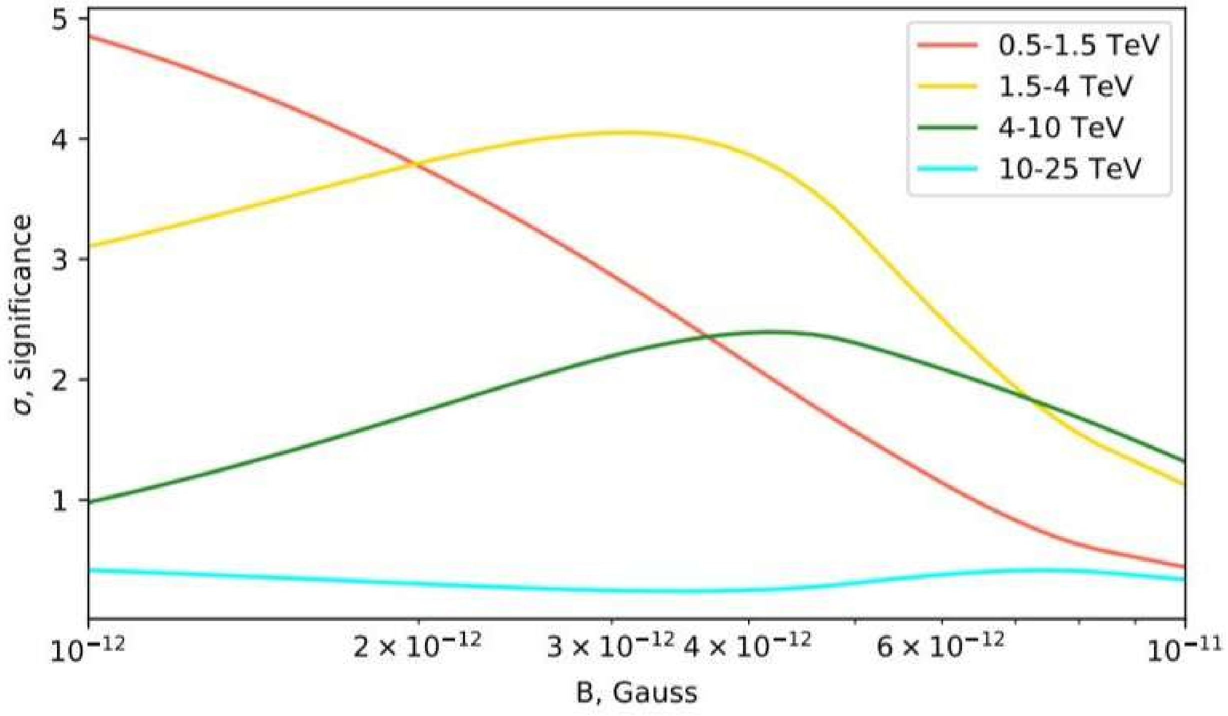

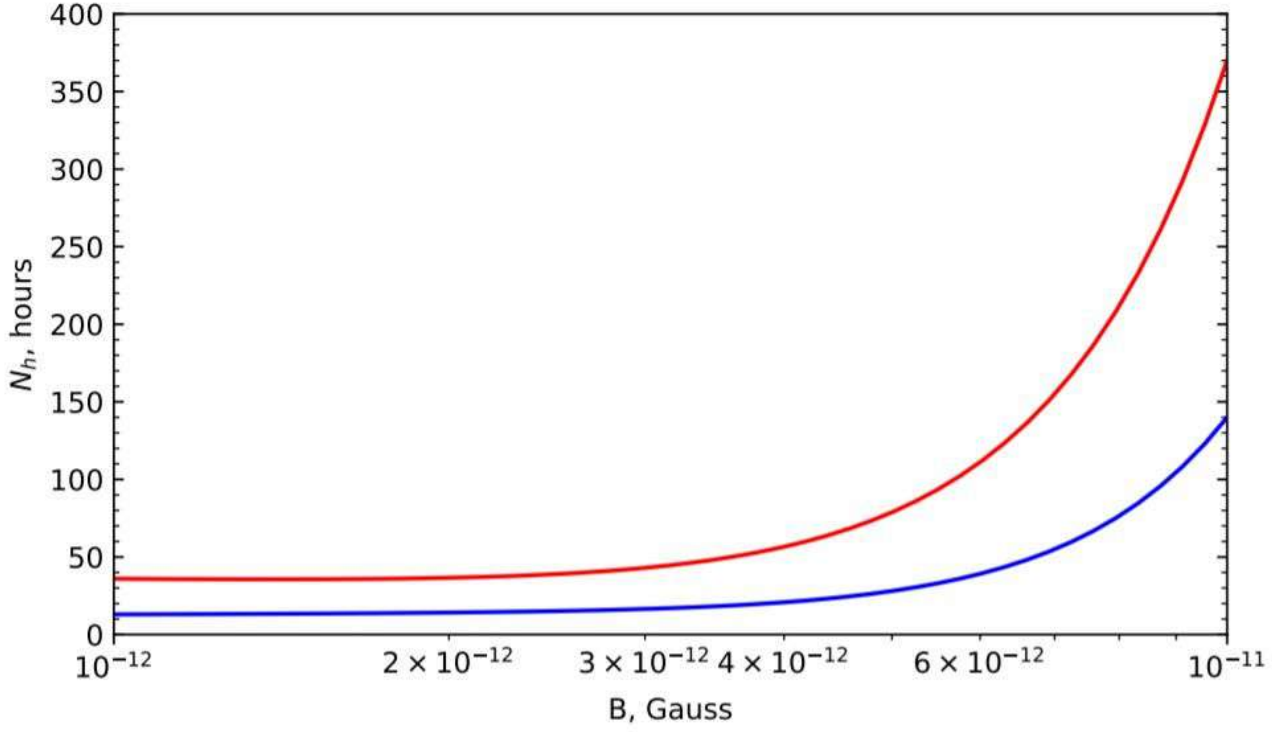

Significance of detection of the extended emission signal in different energy ranges as a function of the assumed magnetic field strength. The assumed exposure of CTA is T = 50 hr.

CTA exposure time needed for 3σ (lower curve) and 5σ (upper curve) detection of the extended emission signal, as a function of IGMF strength.

3σ – 150 hr

Detectability of the IGMF with large correlation length

Detectability of the IGMF with large correlation length

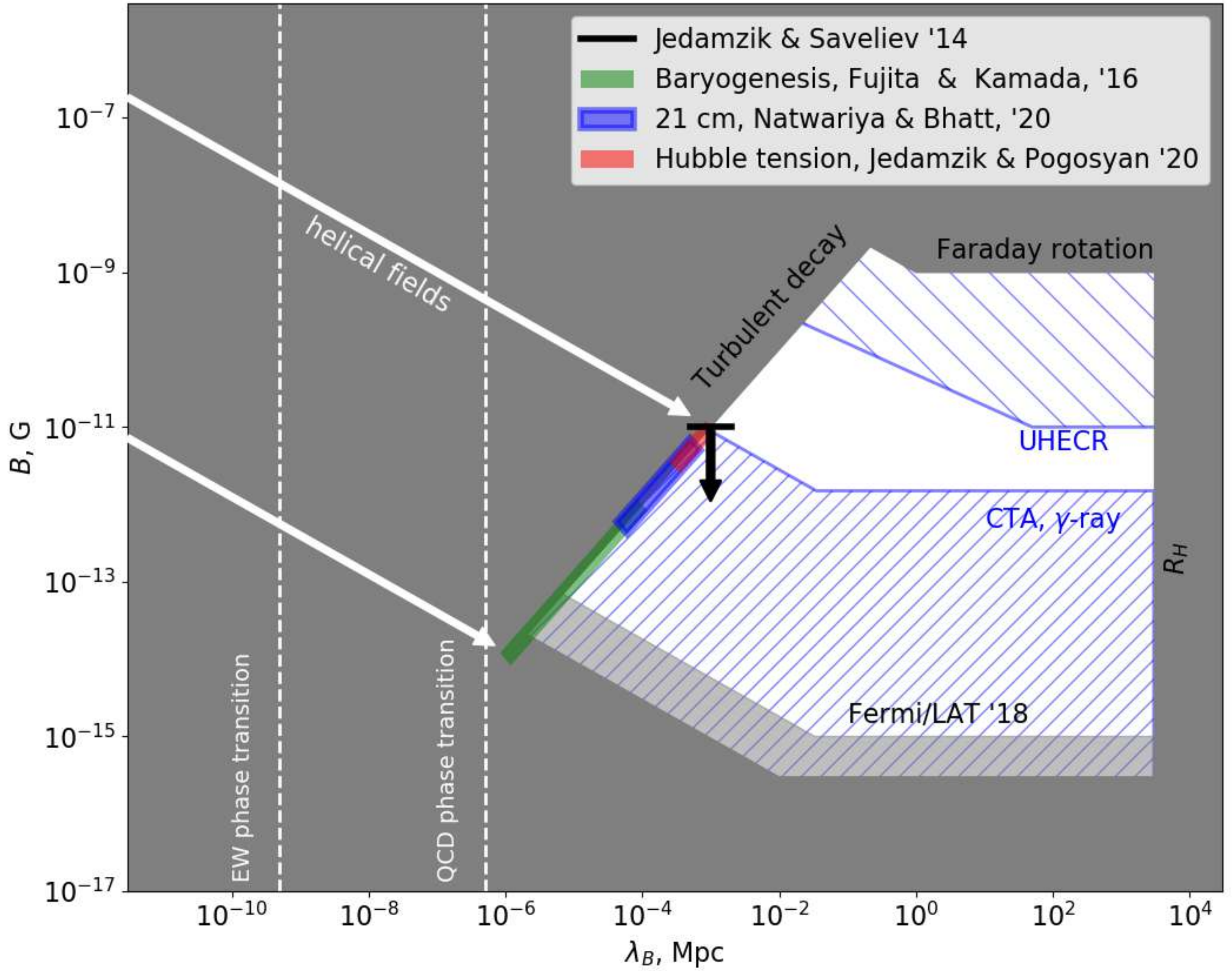

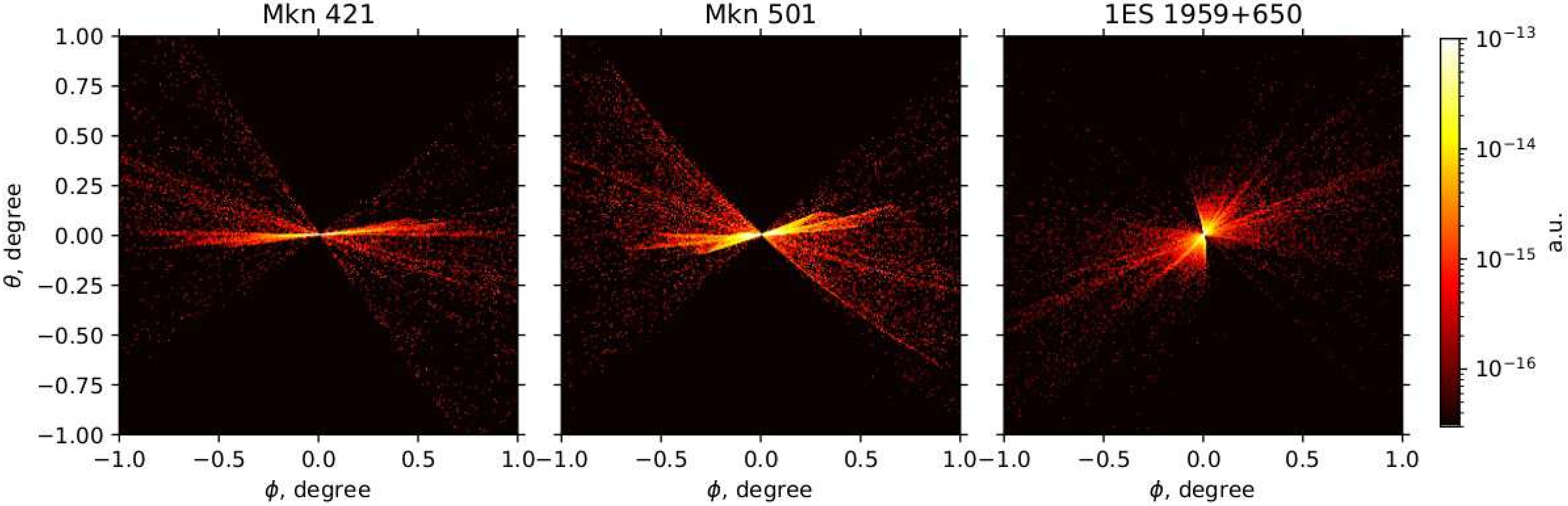

Mkn 421
Mkn 501
1ES 1959+650
θ, degree
ϕ, degree
ϕ, degree
ϕ, degree
a.u.
1.00
0.75
0.50
0.25
0.00
−0.25
−0.50
−0.75
−1.00
−1.0
−0.5
0.0
0.5
1.0
10^{-13}
10^{-14}
10^{-15}
10^{-16}

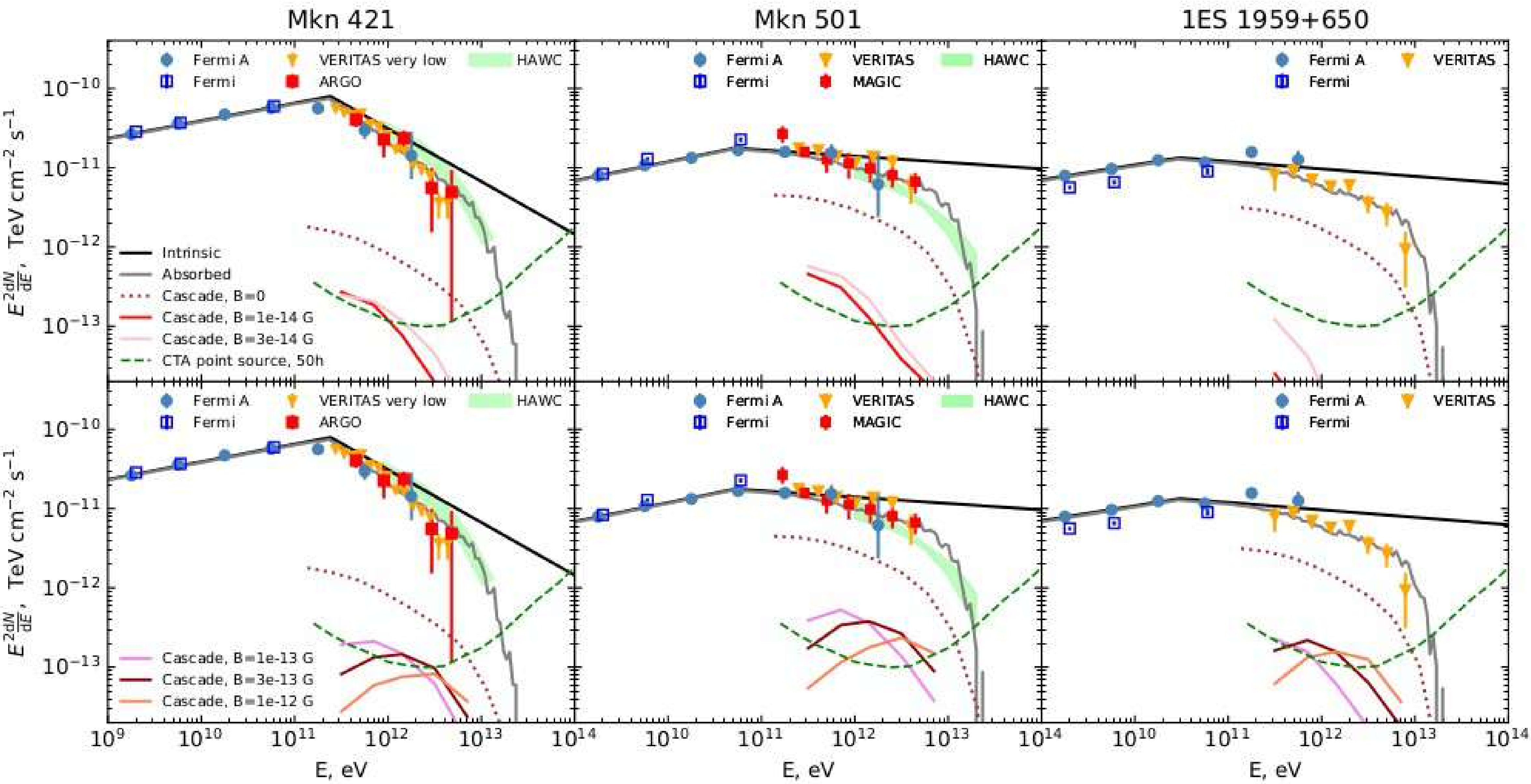

Mkn 421
Mkn 501
1ES 1959+650
Fermi A
Fermi
VERITAS very low
ARGO
HAWC
VERITAS
MAGIC
Intrinsic
Absorbed
Cascade, B=0
Cascade, B=1e-14 G
Cascade, B=3e-14 G
CTA point source, 50h
Cascade, B=1e-13 G
Cascade, B=3e-13 G
Cascade, B=1e-12 G
$E^2\frac{dN}{dE}$, TeV cm^{-2} s^{-1}
E, eV

Local environment effects

Maps of the magnetic fields for two random slices of the TNG100 simulation (20 kpc deep).

Pic from Andres Aramburo Garcia et al, arXiv:2101.07207

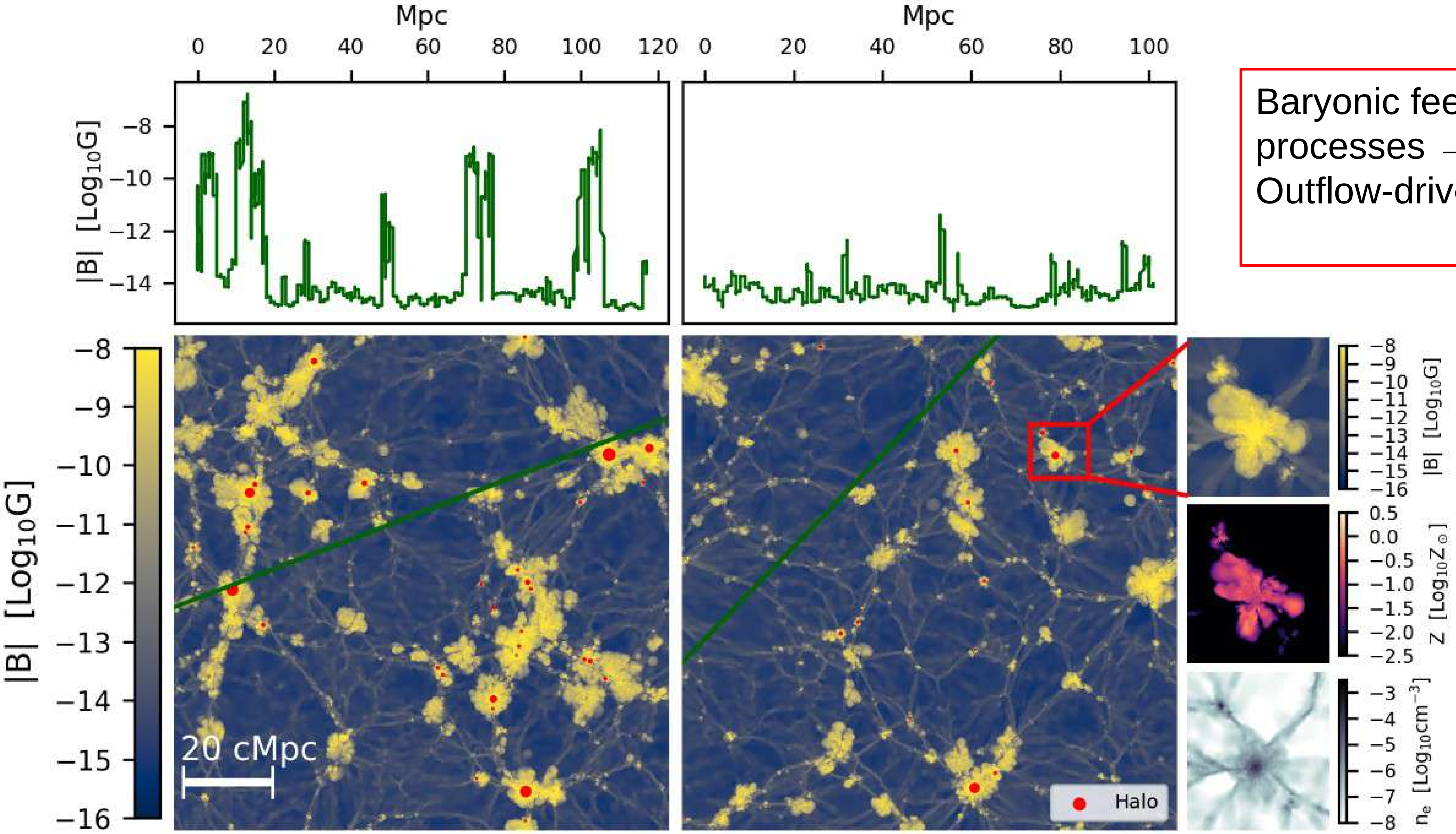

Baryonic feedback processes → Outflow-driven bubbles

What can affect the secondary signal? Local environment near the source

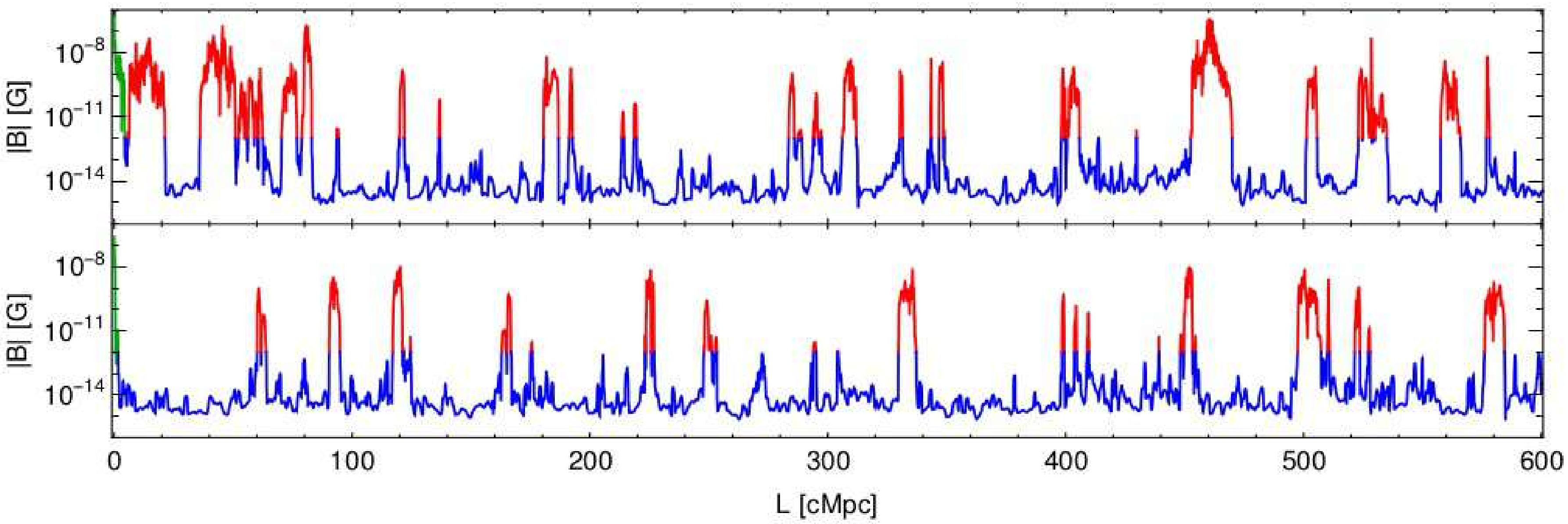

We use the **IllustrisTNG** model to assess the **effect** of contamination of the intergalactic medium by the magnetic field that is spread by the **galactic winds** and its consequences for the measurements of cosmological IGMF

K.Bondarenko, A.Boyarsky, AK, A.Neronov, D.Semikoz, A.Sokolenko
arXiv:2106.02690

- Dark matter density profile along the line of sight toward Mrk 501 based on constained simulation of the LSS

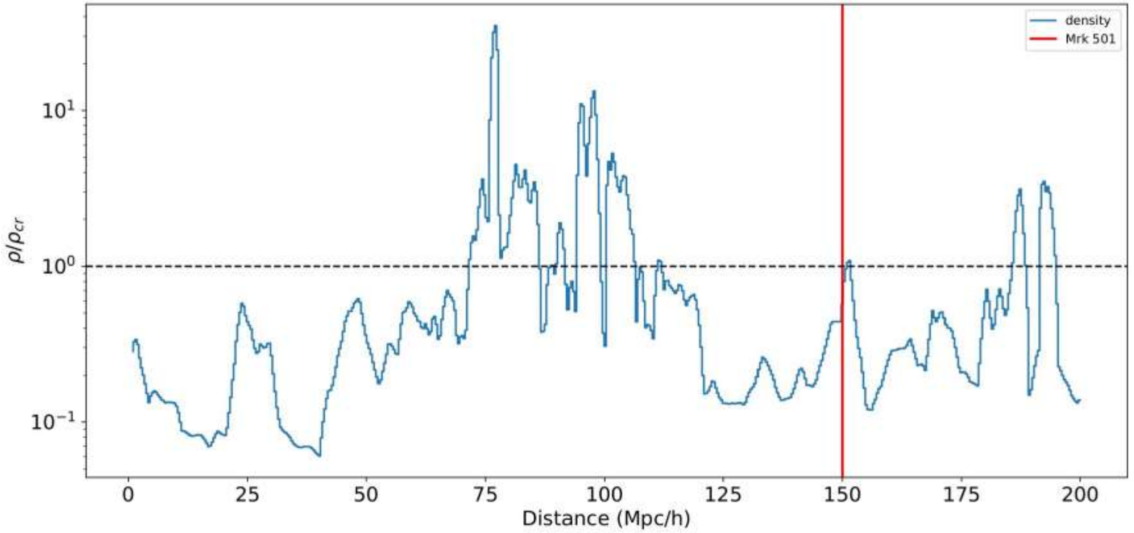

Only voids

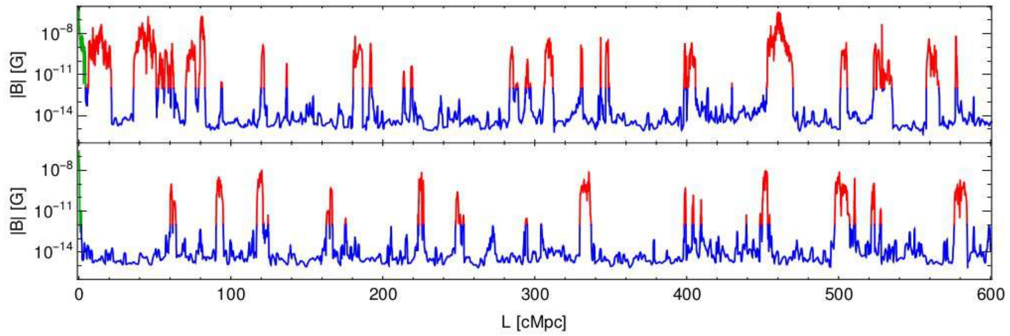

|B| [G]
|B| [G]
L [cMpc]

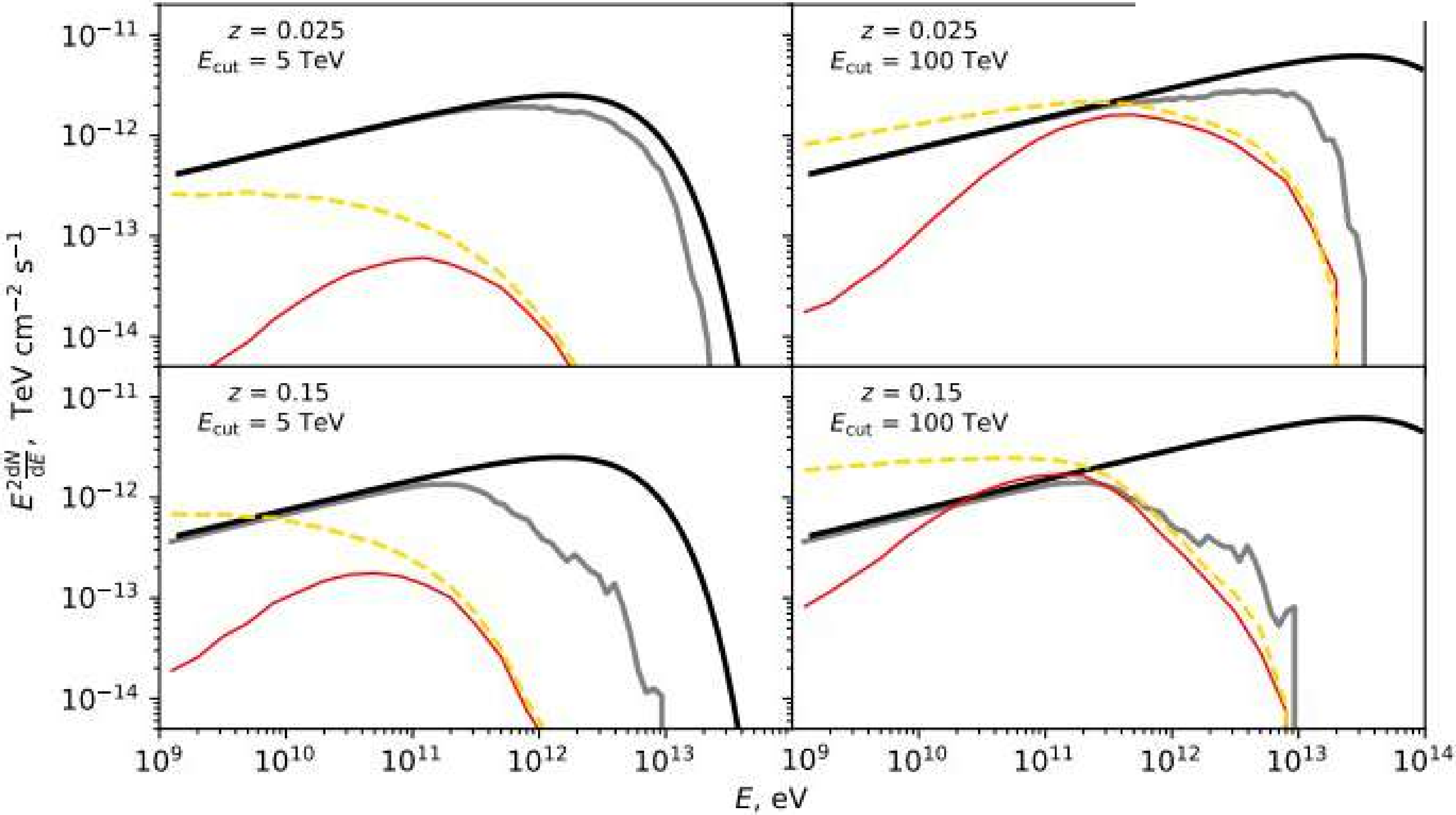

z = 0.025
E_cut = 5 TeV
z = 0.025
E_cut = 100 TeV
z = 0.15
E_cut = 5 TeV
z = 0.15
E_cut = 100 TeV
E^2 dN/dE, TeV cm^-2 s^-1
E, eV

Only first bubble

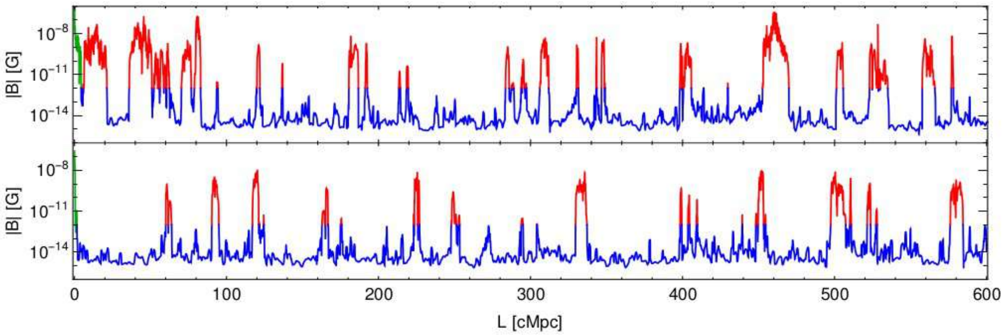

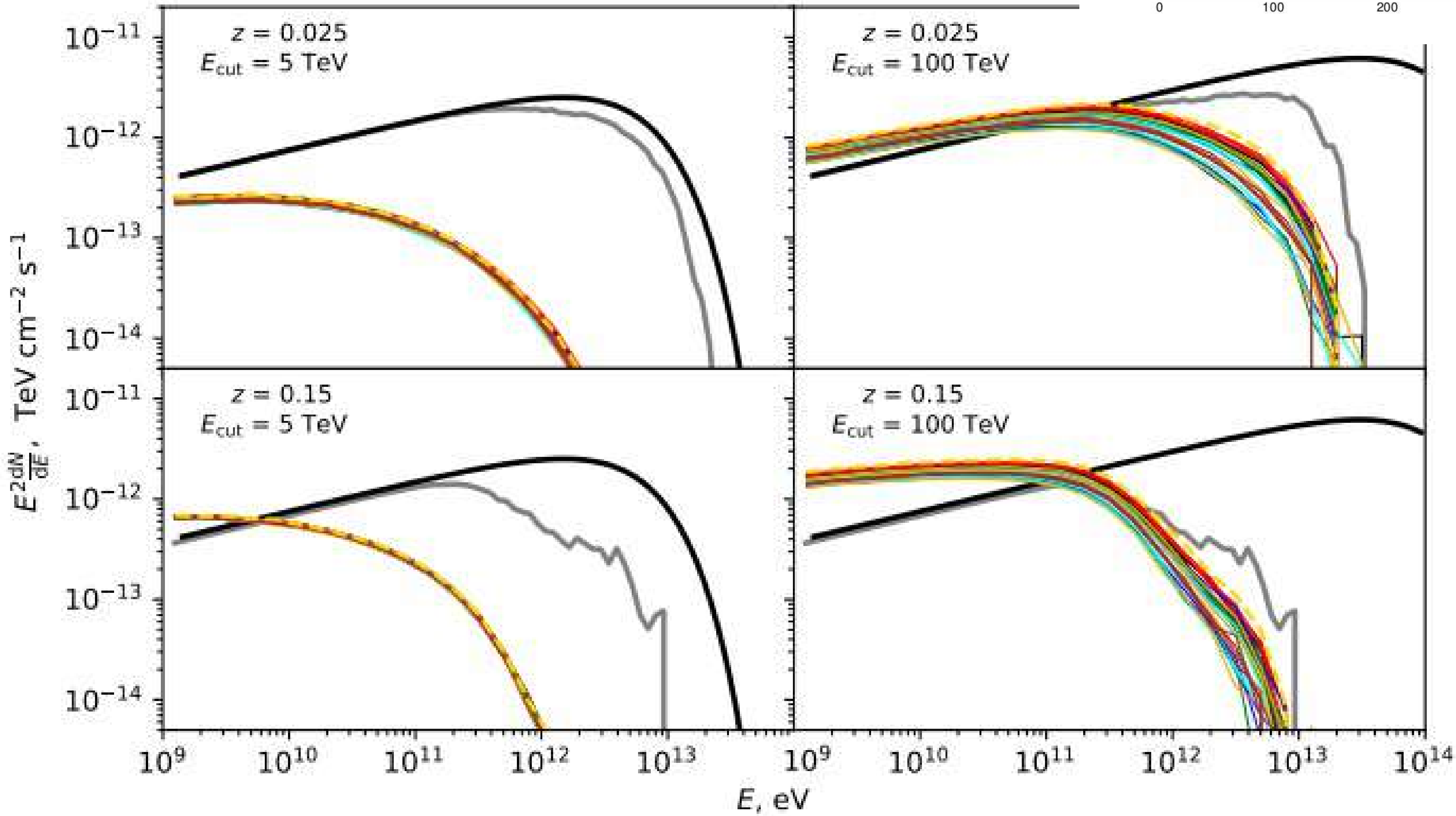

All bubbles without first bubble

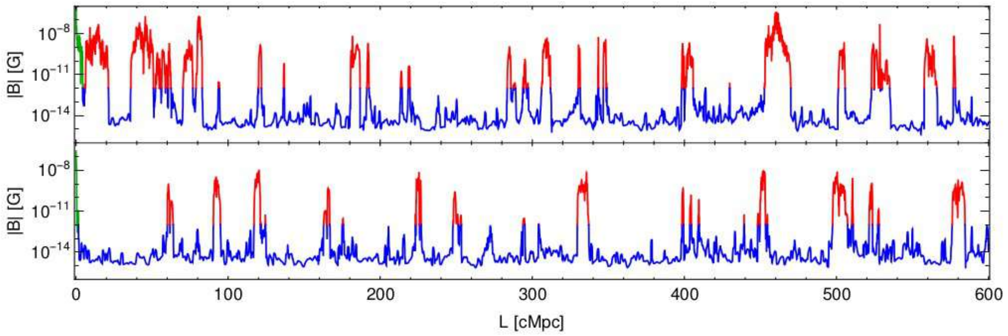

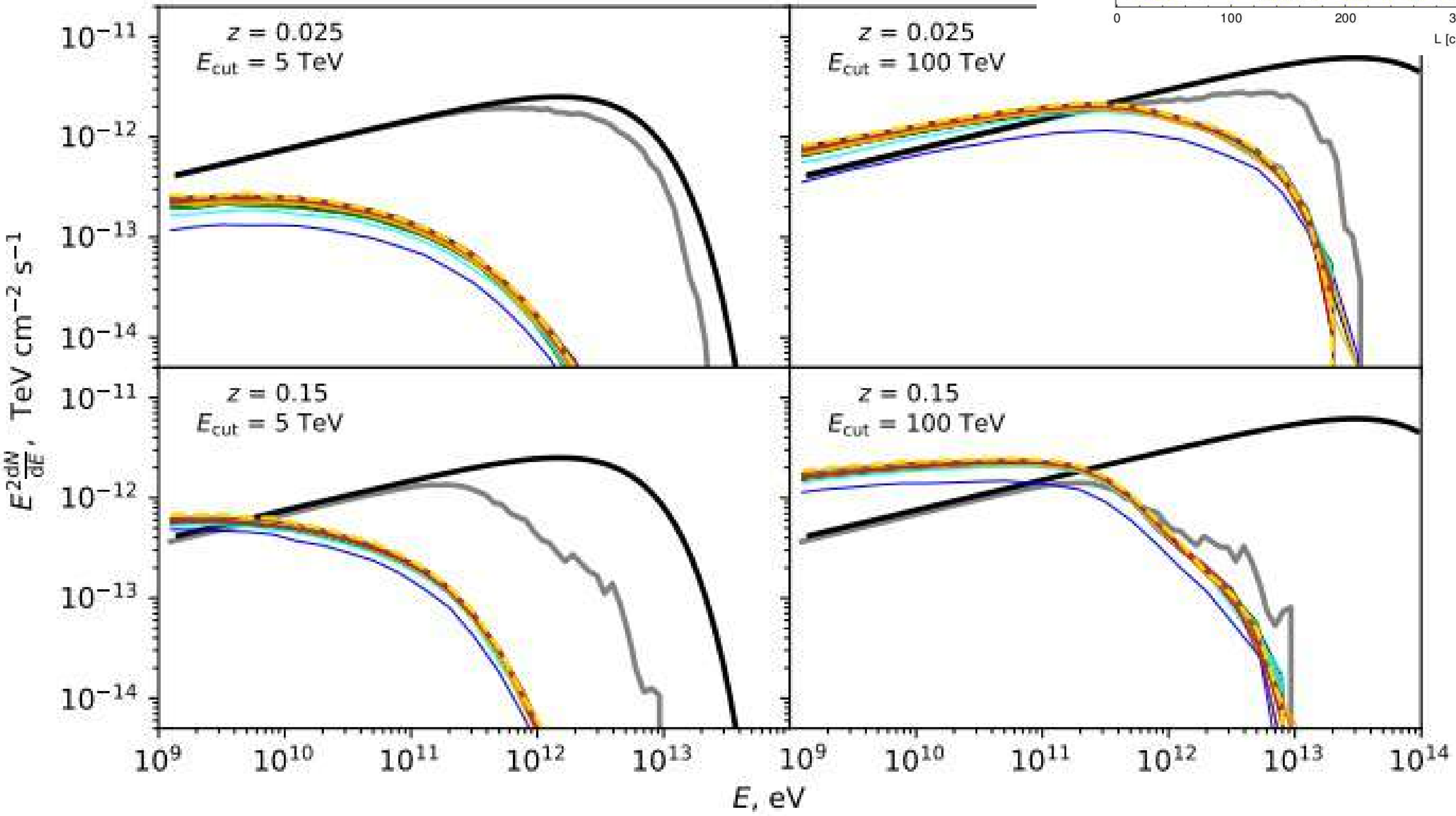

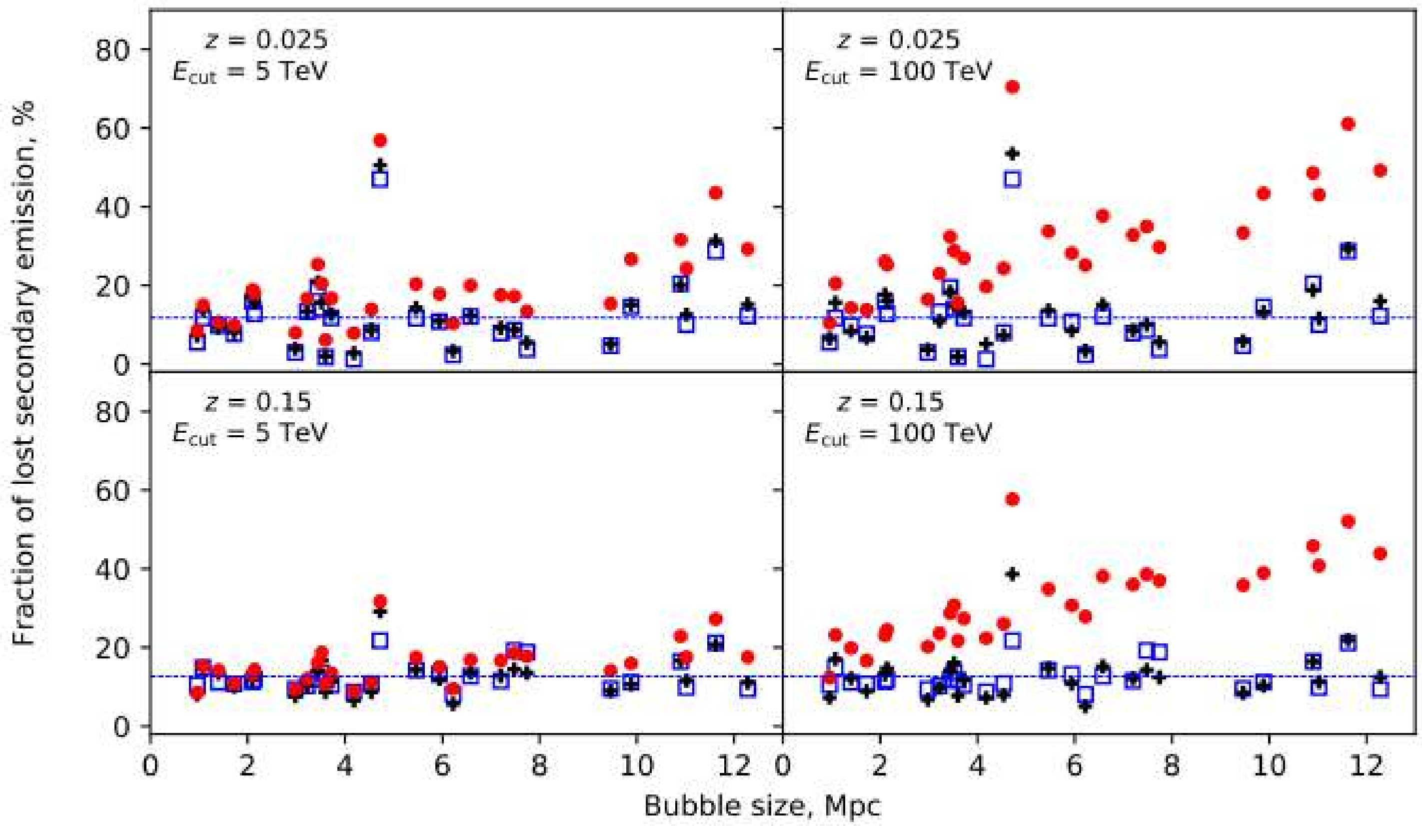

We find that within the IllustrisTNG baryonic feedback model, the **basic features** of the extended or delayed γ-ray signal sensitive to the primordial IGMF are **just slightly altered, typically by 10-20%**. →

This does not preclude the possibility of measuring the primordial field in the voids, but it introduces an **additional systematic uncertainty** that needs to be properly taken into account in the analysis with the future instruments.

What can affect the secondary signal?
Errors in Monte Carlo codes

Comparison of the CRPropa, ELMAG and CRbeam gamma-ray propagation codes

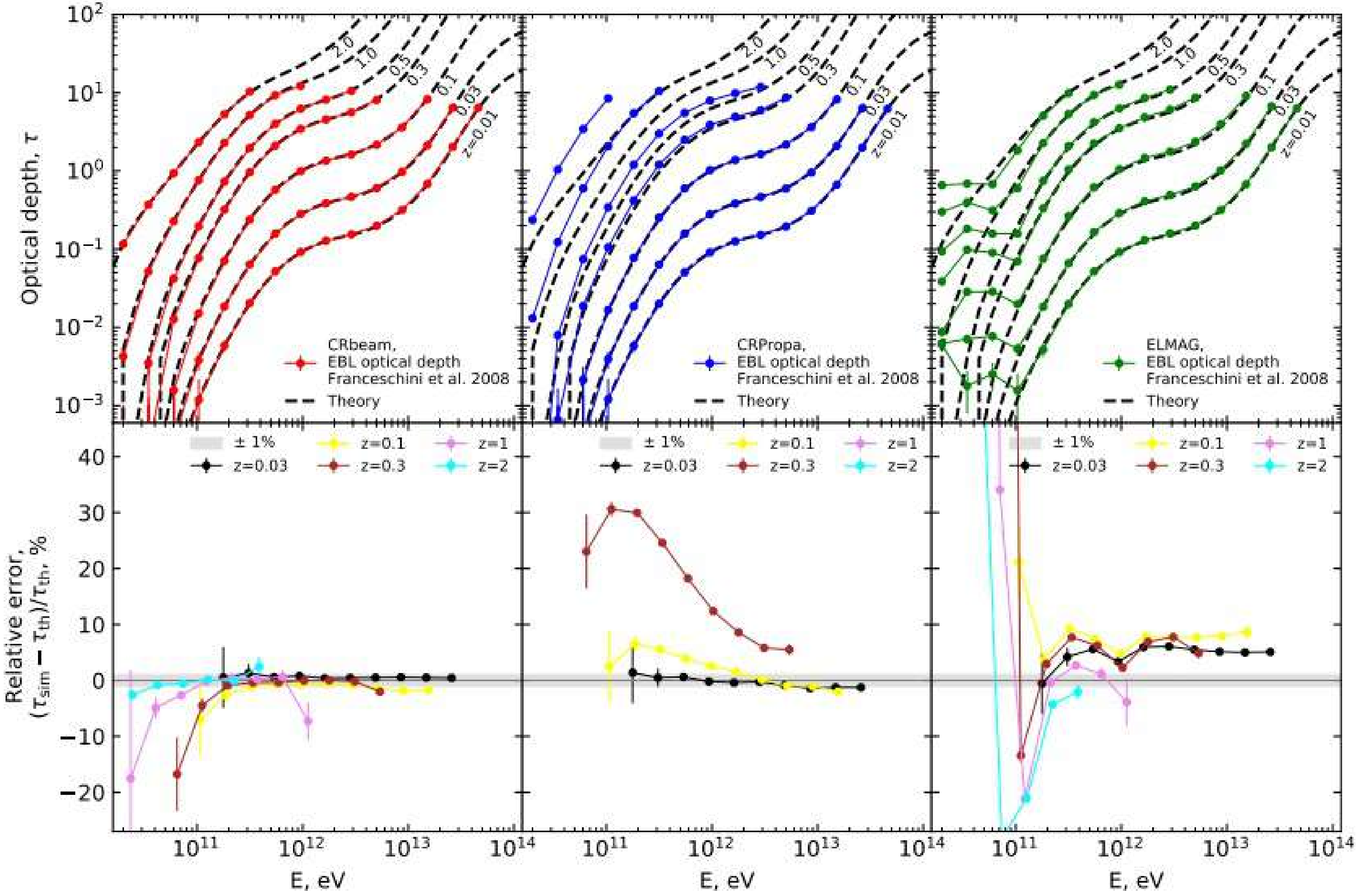

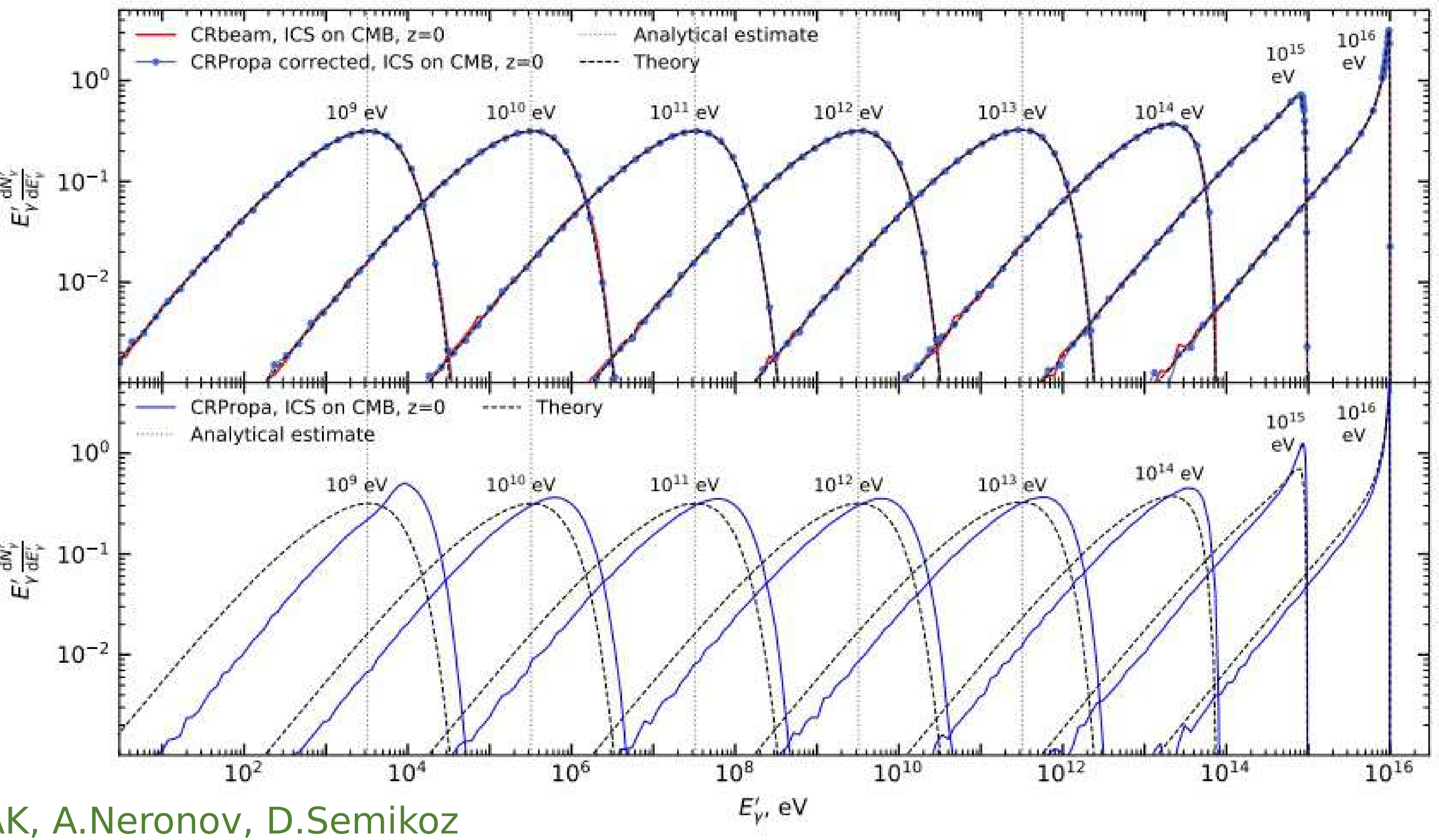

O.Kalashev, AK, A.Neronov, D.Semikoz

arXiv:2201.03996

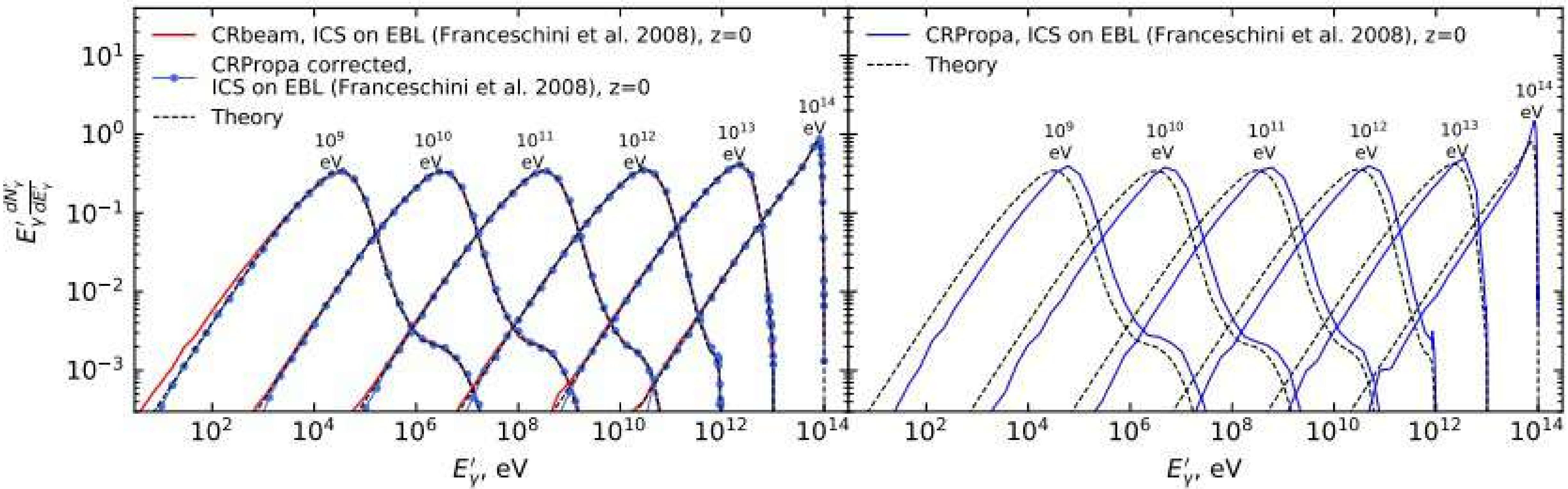

CRbeam, ICS on EBL (Franceschini et al. 2008), z=0
CRPropa corrected,
ICS on EBL (Franceschini et al. 2008), z=0
Theory
CRPropa, ICS on EBL (Franceschini et al. 2008), z=0
Theory
$E'_\gamma \frac{dN'_\gamma}{dE'_\gamma}$
E'_γ, eV
E'_γ, eV
10^9 eV
10^{10} eV
10^{11} eV
10^{12} eV
10^{13} eV
10^{14} eV

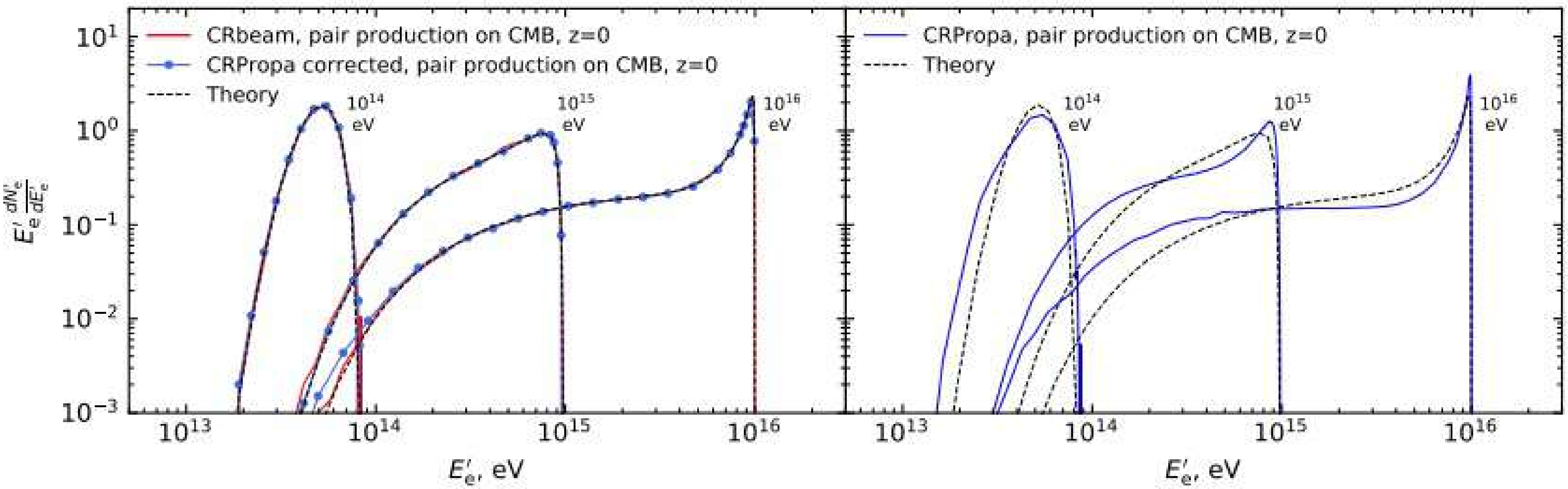
CRbeam, pair production on CMB, z=0
CRPropa corrected, pair production on CMB, z=0
Theory
CRPropa, pair production on CMB, z=0
Theory
10^{14} eV
10^{15} eV
10^{16} eV
$E'_e \frac{dN'_e}{dE'_e}$
$E'_{e'}$, eV
$E'_{e'}$, eV

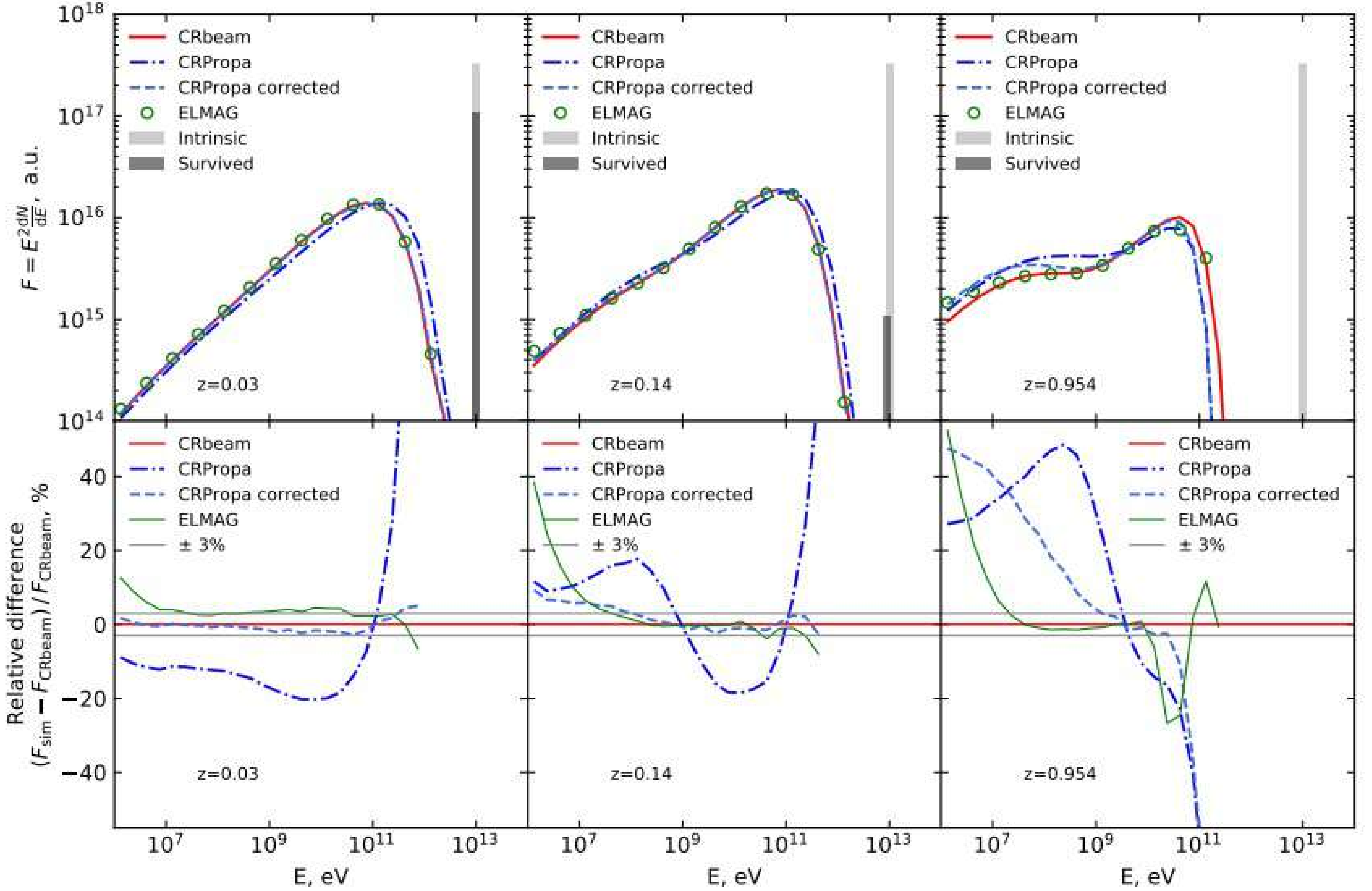
CRbeam
CRPropa
CRPropa corrected
ELMAG
Intrinsic
Survived
z=0.03
z=0.14
z=0.954
± 3%
$F = E^2\frac{dN}{dE}$, a.u.
Relative difference
$(F_{\rm sim} - F_{\rm CRbeam})\,/\,F_{\rm CRbeam}$, %
E, eV

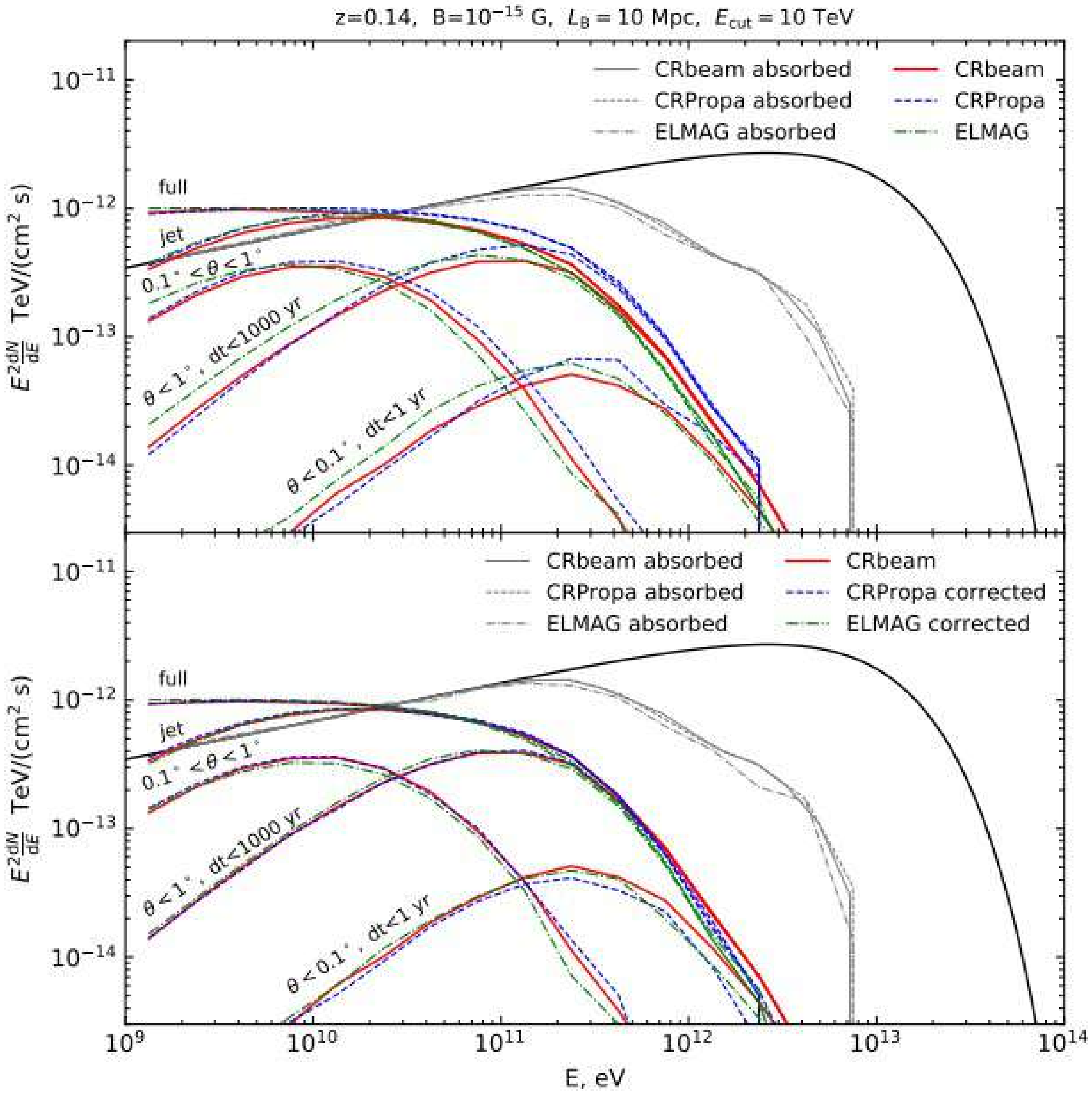

z=0.14, B=10^−15 G, L_B = 10 Mpc, E_cut = 10 TeV
CRbeam absorbed
CRPropa absorbed
ELMAG absorbed
CRbeam
CRPropa
ELMAG
CRPropa corrected
ELMAG corrected
full
jet
0.1° < θ < 1°
θ < 1°, dt<1000 yr
θ < 0.1°, dt<1 yr
E^2 dN/dE TeV/(cm^2 s)
E, eV

What can affect the secondary signal? AGN duty cycle

14 years of observations of 1ES 0229 with Fermi/LAT, MAGIC, VERITAS and HESS

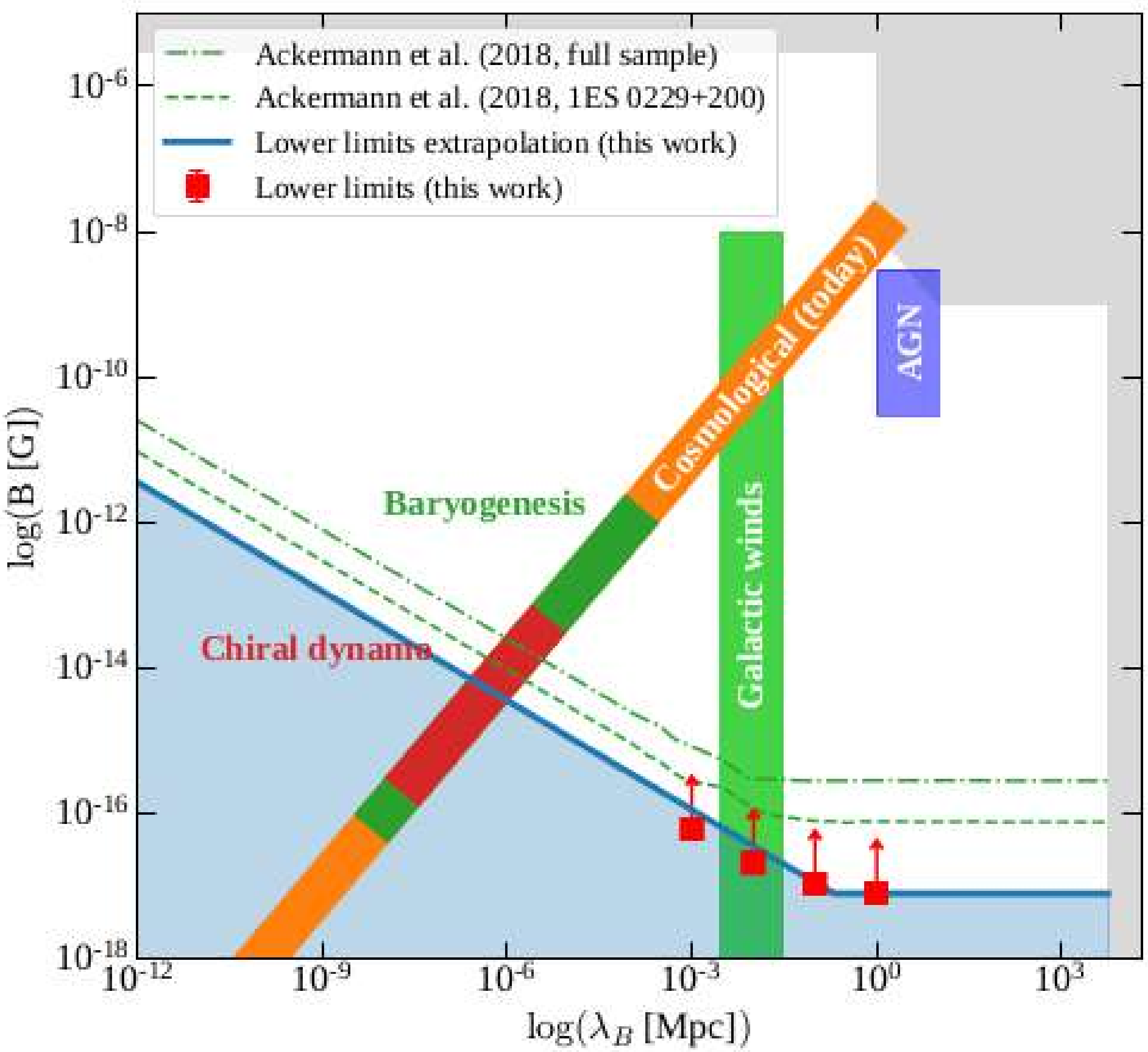

AK and D.Semikoz for the MAGIC collaboration

Internal review in the MAGIC

Thank you for your attention

EBL

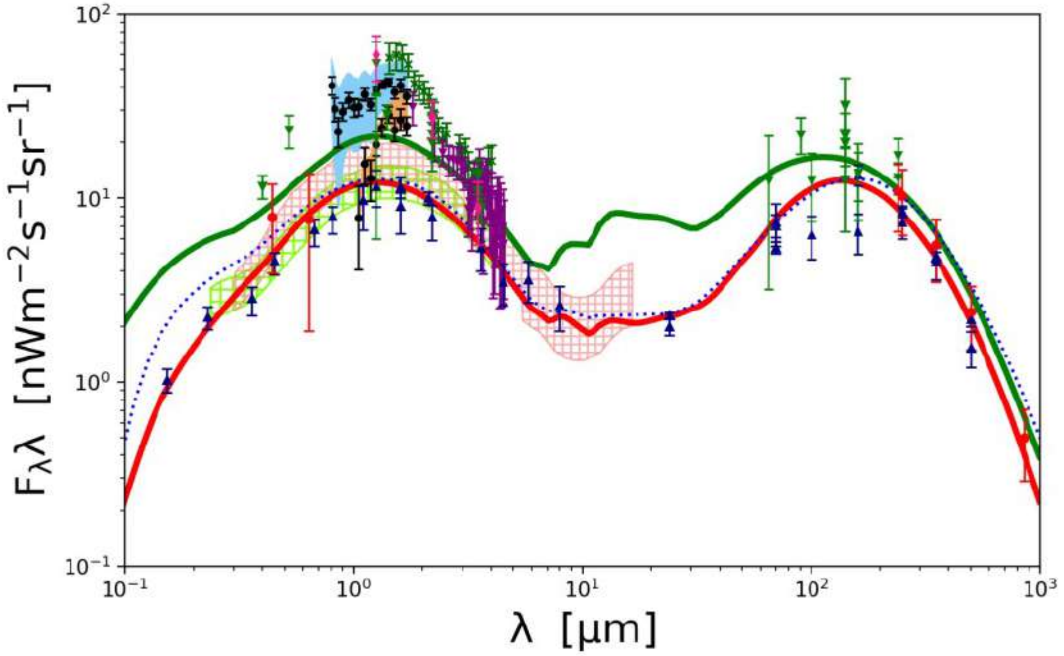

A.Korochkin, G.Rubtsov, arXiv: *1712.06579*

Background: long-standing contradiction between direct observations of the EBL and constraints from gamma-ray measurements and galaxy counts

Idea: use direct measurements as an upper limits,
galaxy counts as a lower limits
and constrain astrophysical parameters of the EBL based on allowed range of EBL intensities

Method: for the first time we develop a numerical model of the EBL spectrum while maintaining the explicit dependence on the astrophysical parameters involved.

We constructed a Markov Chain to explore the parameter space. The posterior distributions built with the Markov Chain Monte Carlo method are used to determine an allowed range of the individual parameters of the model.

Results: constraints on star formation rate, initial mass function, parameters of giant molecular clouds. Constraints are comparable to those presented in the literature.

EBL

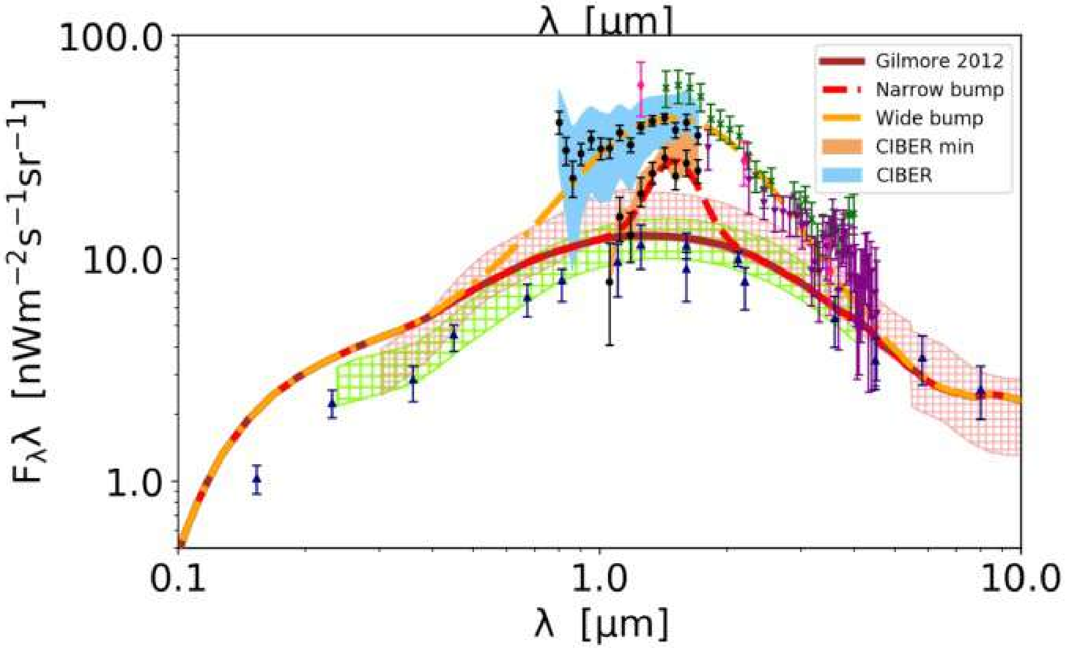

Background: long-standing contradiction between direct observations of the EBL and constraints from gamma-ray measurements and galaxy counts

Idea: discrepancies of the measurements with different methods could be due to the presence of features in the EBL spectrum that are localised in the micron wavelength range.

Measurements of the EBL from the γ-ray data conventionally adopt assumptions about the shape of the EBL spectrum and thus insensitive to narrow spectral features.

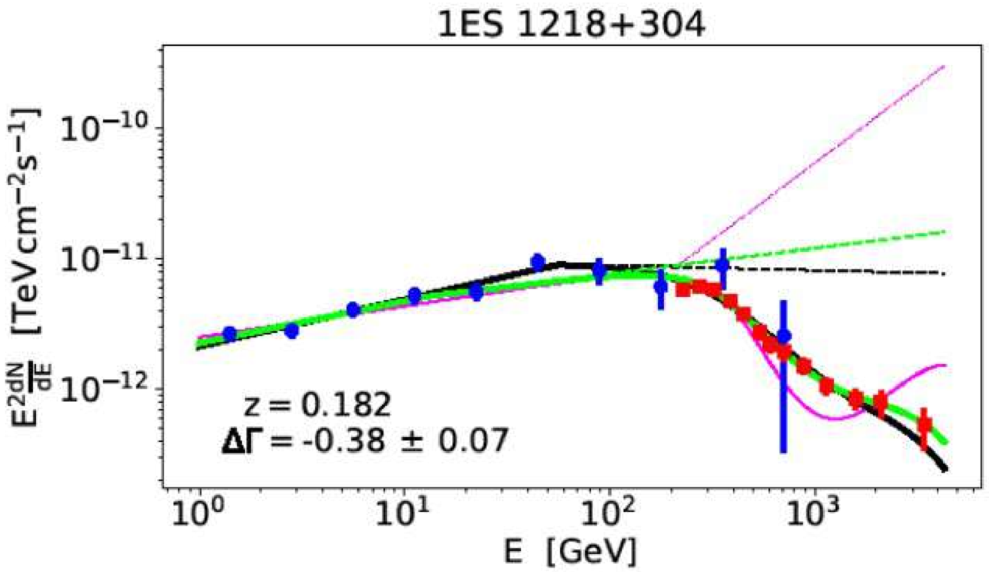

Method: we use combined Fermi/LAT and IACT data to search for imprints of the bump in the blazar spectra.

Results: we show that a previously reported 'excess' in EBL flux in the ∼ 1 micron wavelength range is consistent with gamma-ray measurements, that is, if the excess has the form of a narrow feature of the width $\delta\lambda < \lambda$ and an overall flux of up to 15 nW/(m 2 sr) above the 'minimal' EBL, which is estimated from the visible and infrared source counts.

Such 'bump-like' spectral features could originate, for example, from decaying dark-matter particles, or either axions or peculiar astrophysical processes in the course of star-formation history.

We show that CTA will be able to detect such a feature with high significance.

A.Korochkin, A.Neronov, D.Semikoz, arXiv: *1906.12168*

ALPs

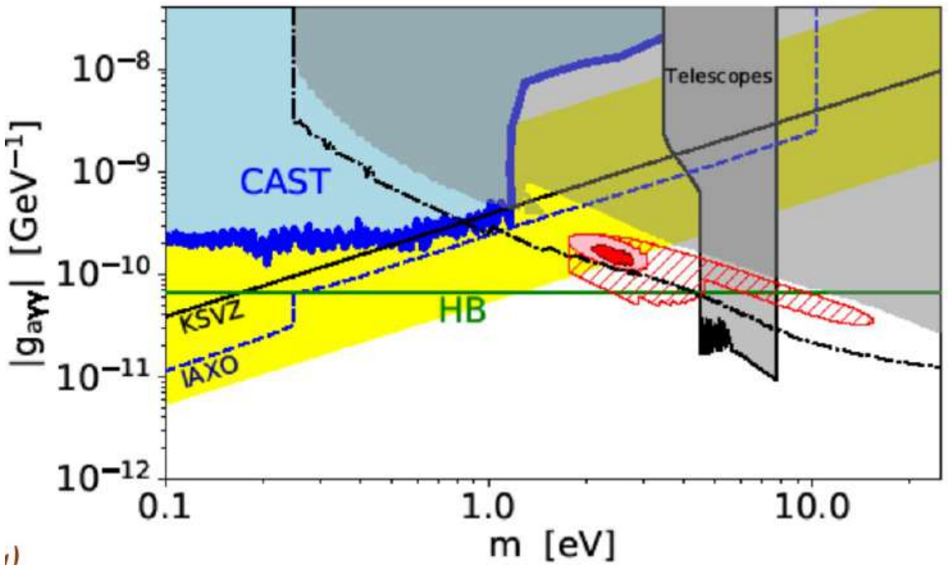

A.Korochkin, A.Neronov, D.Semikoz,
arXiv: *1911.13291*

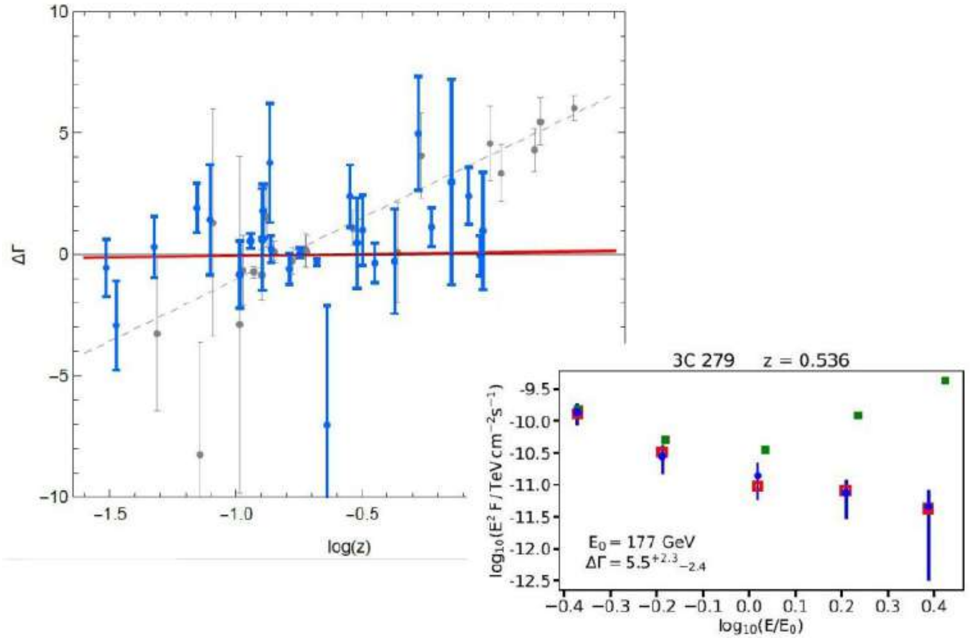

AK,G.Rubtsov,S.Troitsky,
arXiv:*1810.03443*

Idea: bump in the EBL spectrum from previous chapter could be due to decay of ALPs with mass ~1 eV constituting dark matter

Hence gamma-ray observations can be used to limit ALP-two-photon coupling.

Results: We found 95% C.L. limit on axion-like particle mass and coupling constant from non-observation of ALP decay bump in EBL spectrum, using gamma-ray spectrum of the blazar 1ES 1218+304 observed by Fermi/LAT and VERITAS telescopes (grey shading). Our best fit model favours non-zero amplitude of the ALP induced absorption feature in the γ-ray spectrum (red striped region).

CTA and LHAASO will be able to detect the ALP induced bump with high significance, and provide precision measurement of the ALP mass and photon coupling constant (black dot-dashed line).

“anomalous transparency” – appearance of upward breaks in the deabsorbed spectra (Horns Meyer 2012, Rubtsov Troitsy 2014).

Based on the most complete sample of blazars with accurately measured redshifts, we have shown that the significance of the “anomalous transparency” effect is weaker than previously reported and does not exceed 2σ for the modern EBL models and even as low as 1.3σ for the most conservative EBL model of Gilmore 2012.

The results of previous works relied on sources with incorrect redshifts, biased method of deabsorption and wrong treatment of uncertainties (gaussian vs poissonian).

Положения, выносимые на защиту

1. Разработана новая модель межгалактического фонового излучения, позволяющая модифицировать параметры астрофизических процессов, лежащих в ее основе. На основе данной модели установлены ограничения на скорость звездообразования во Вселенной.

2. Показано, что эффект “аномальной прозрачности” Вселенной для гамма-излучения высоких энергий слабее, чем считалось ранее и его значимость составляет 1.3σ для наиболее консервативной модели поглощения.

3. Установлены ограничения на положение, ширину и интенсивность небольшой, локализованной в области длин волн порядка микронов, добавки на фоне теоретически предсказанного спектра межгалактического фонового излучения.

4. На основе наблюдений высокоэнергичного излучения блазаров установлены ограничения на константу взаимодействия с фотонами g гипотетических аксионоподобных частиц с массой в области 1 эВ при условии, что они составляют большую часть темной материи.

5. Рассчитана чувствительность гамма-телескопа нового поколения CTA к внегалактическим магнитным полям. Было показано, что метод измерения гамма-излучения позволяет детектировать сильные первичные магнитные поля с напряженностью в области 10^{-12} Гс – 10^{-11} Гс.

6. Установлено, что типичные пузыри магнитного поля вокруг галактик и скоплений галактик, соответствующие модели IllustrisTNG, вызывают энергонезависимое подавление потока вторичных гамма-квантов на уровне около 10%.